

2022年1月13日@SPring-8次世代先端研究会

SPring-8先端利用技術ワークショップ



広島大学



Research Institute
for Nanodevice
& Bio Systems

RNBS

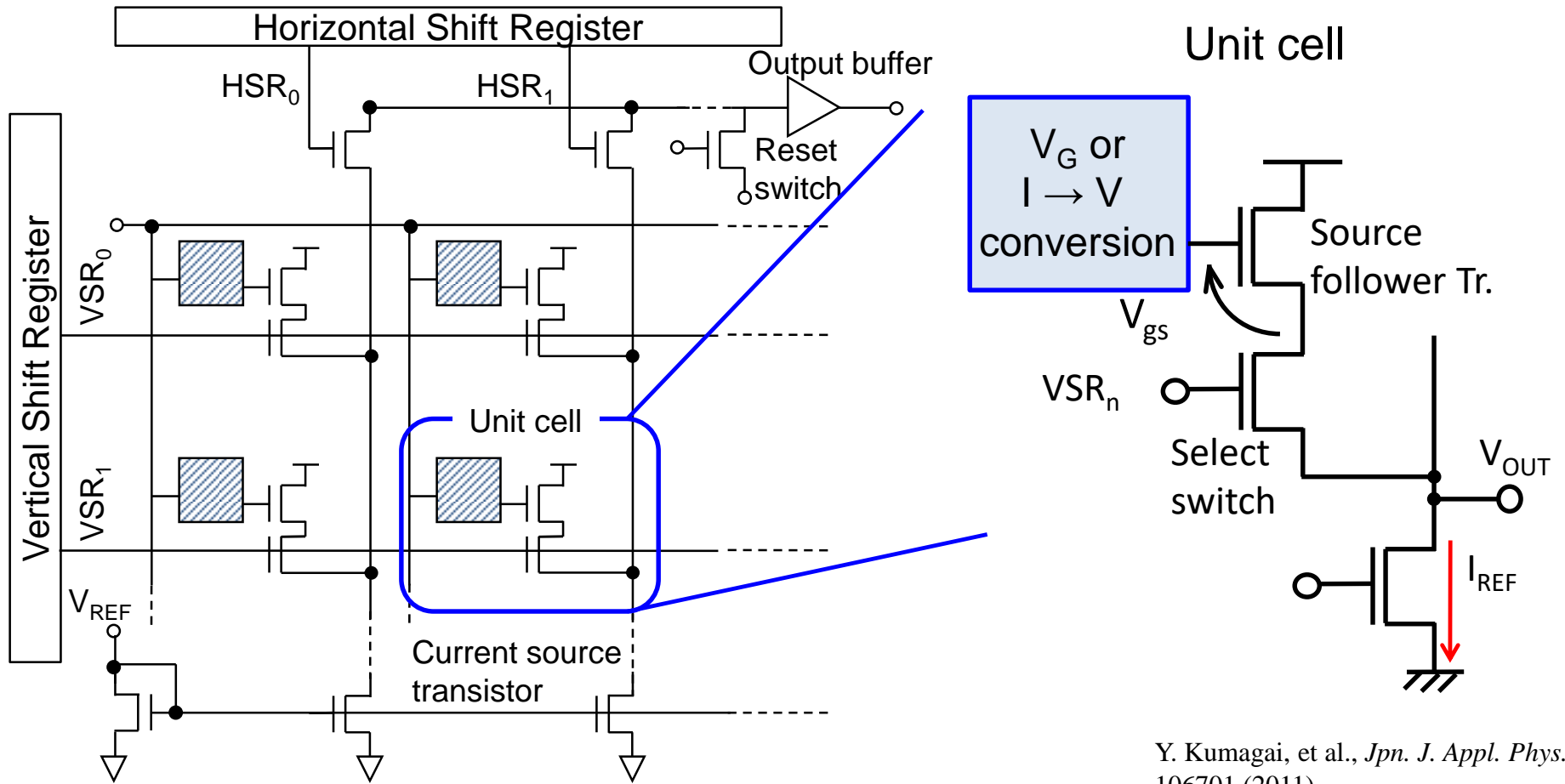
集積回路における半導体トランジスタ のバラツキ・雑音について

広島大学ナノデバイス・バイオ融合科学研究所

所長・教授 寺本 章伸

Measurement method

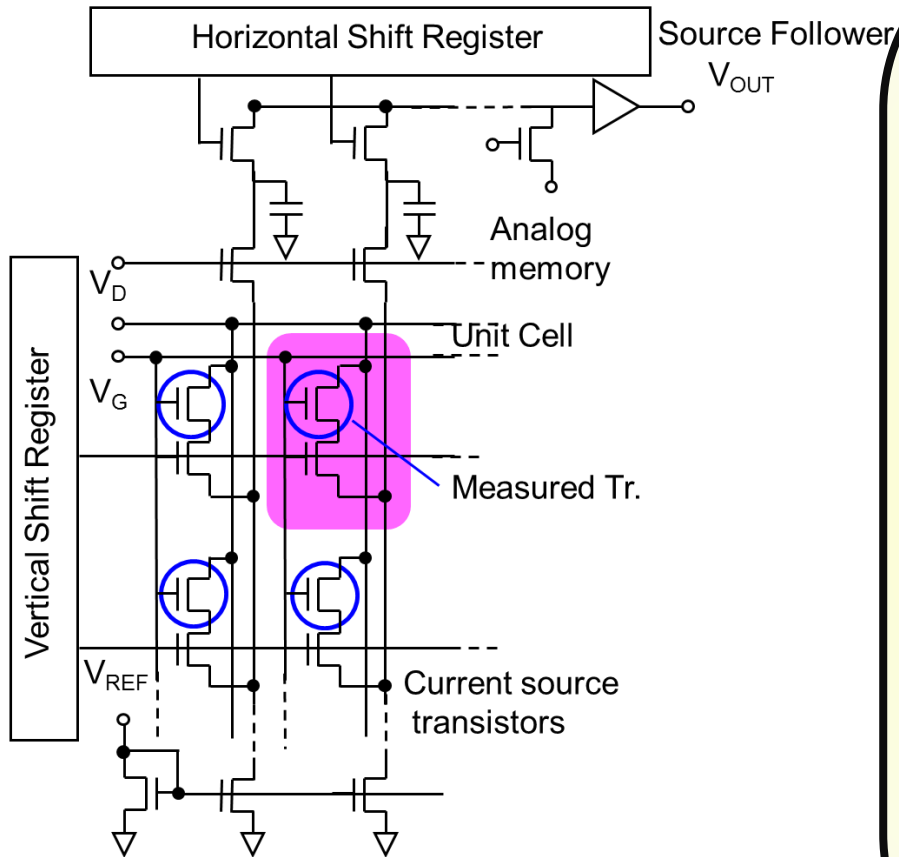
基本的なテスト回路



Y. Kumagai, et al., *Jpn. J. Appl. Phys.*, 50, 106701 (2011)

ソースフォロア回路によって回路内で電流を電圧信号に変換
電圧信号は増幅された後、外部に出力

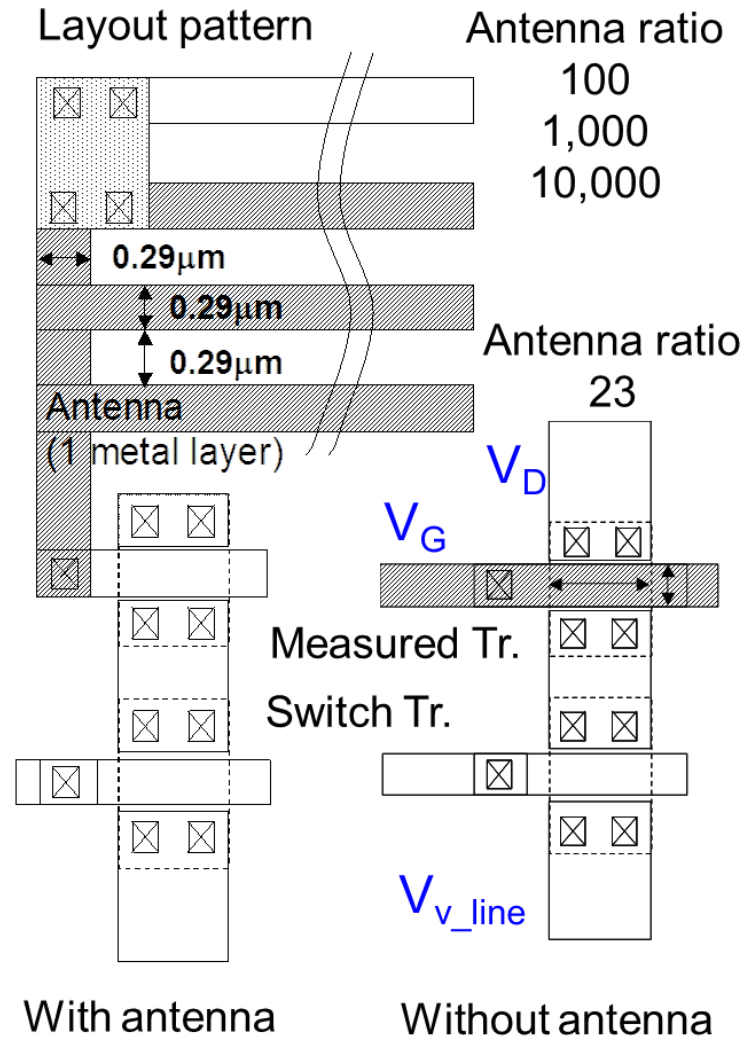
Circuit schematic view of test structure



- Arrayed measured Tr. and select switch Tr.
⇒ easy to integrate many Trs.
- Simple peripheral circuit
⇒ operating in a wide range to measure various Trs. with L, W, gate insulator, its thickness,...
- Read-out and charging vertical line in parallel
⇒ rapid measurement

Test Structure

Process	0.22 μ m 1-poly 2-metal standard CMOS process
Number of Tr.	1,258,816 (nMOS) 786,760 (pMOS)
Number/ 1 size	131,072 81,920
Type of Tr.	21
	nMOS, pMOS
Unit cell area	5 μ m \times 5 μ m (nMOS) 7.5 μ m \times 5 μ m (pMOS)
Reading time	0.7sec/shot
TEG size	5.5 \times 14 mm ²
Pad number	16

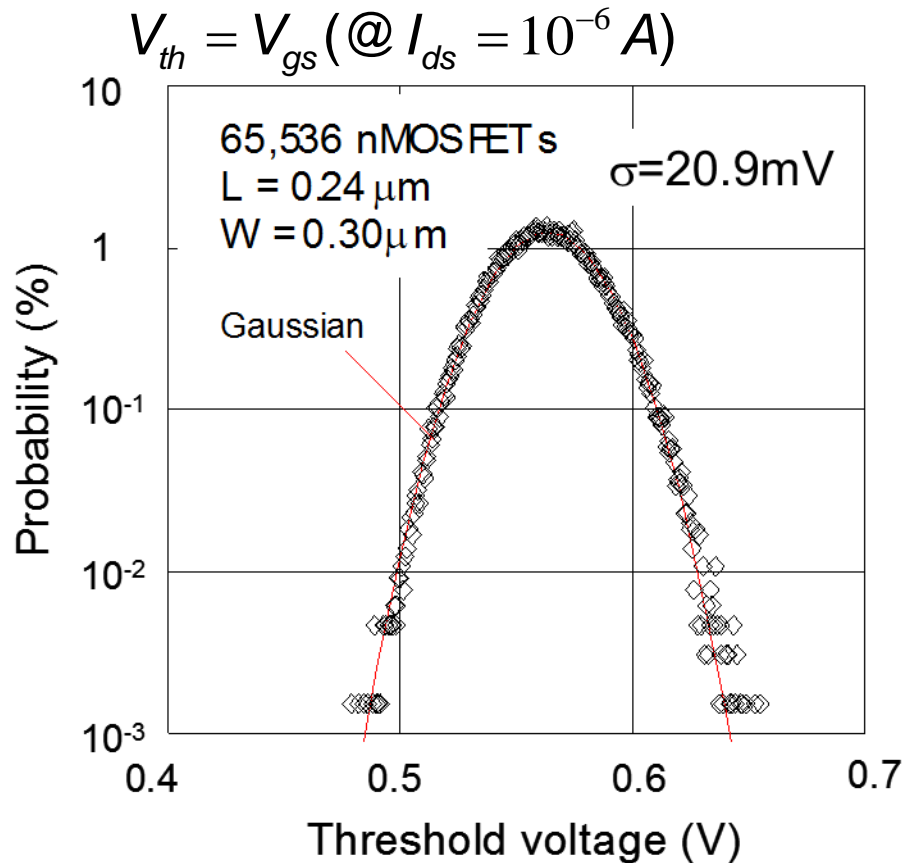


It is possible to measure various type MOSFETs

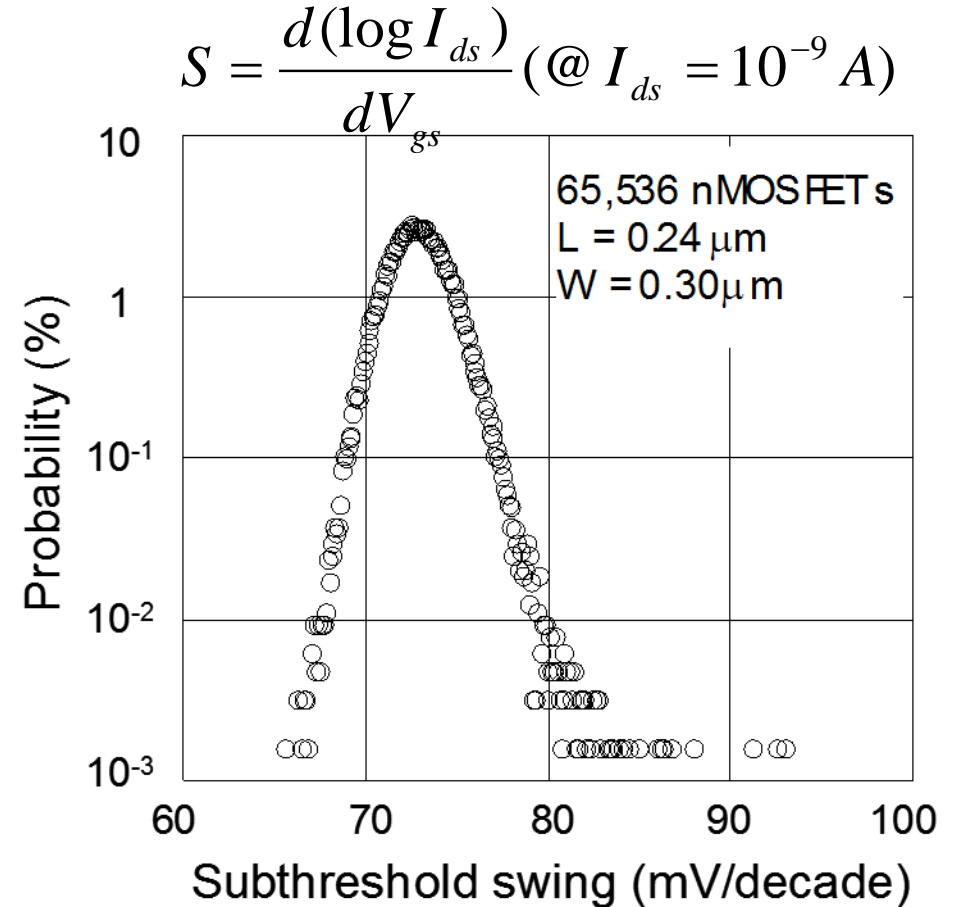
MOSFETの特性ノバラツキ

Distribution of threshold voltages and S-factors

Threshold voltage



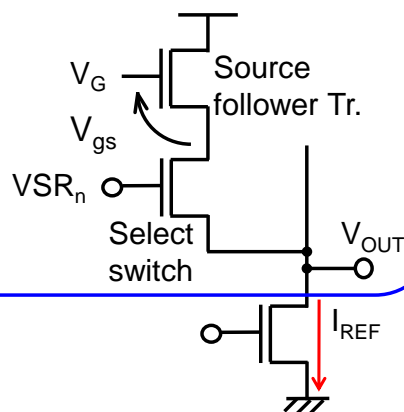
Subthreshold swing



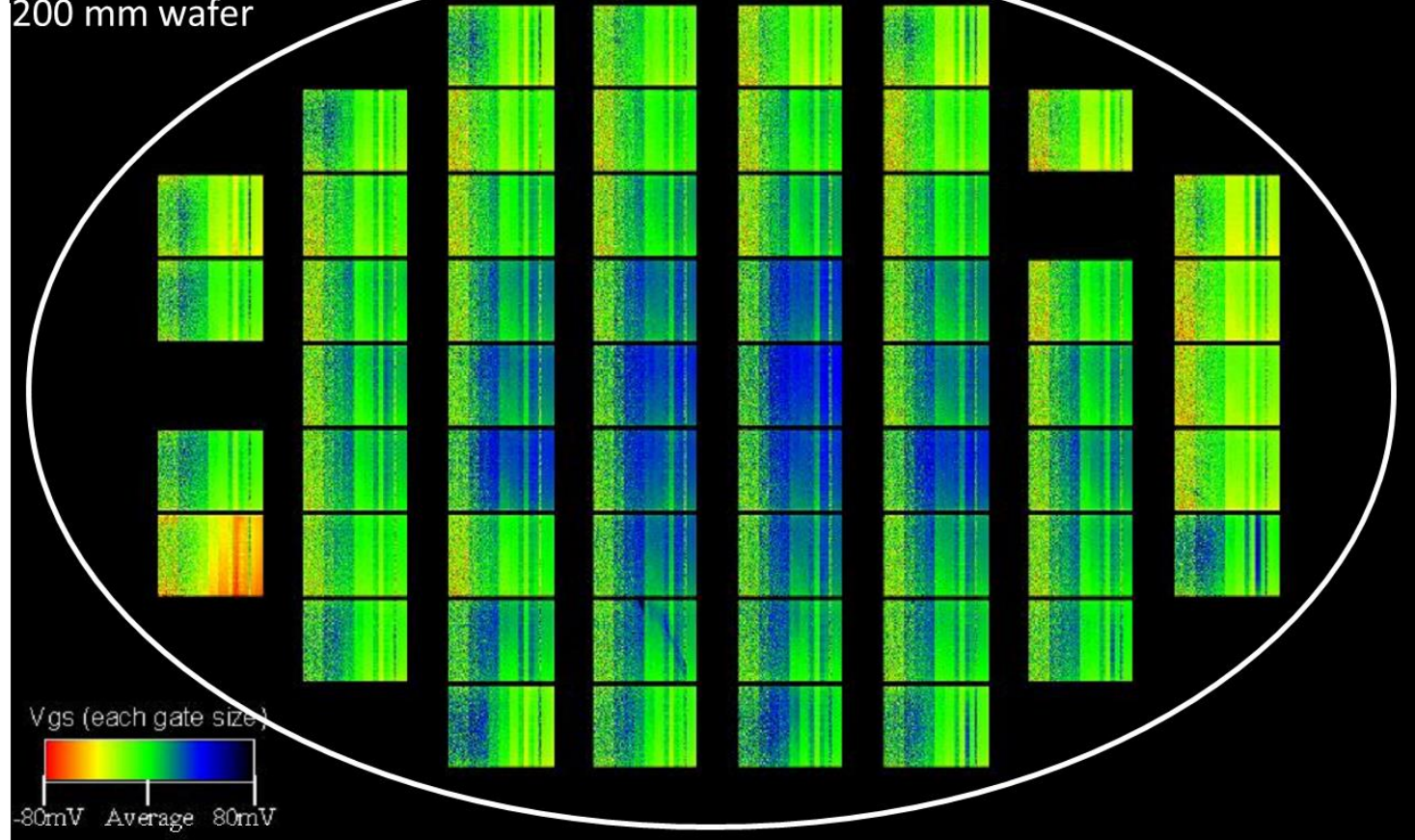
We can evaluate distribution of V_{th} and S-factor easily.

Wafer Map of V_{th}

Unit cell



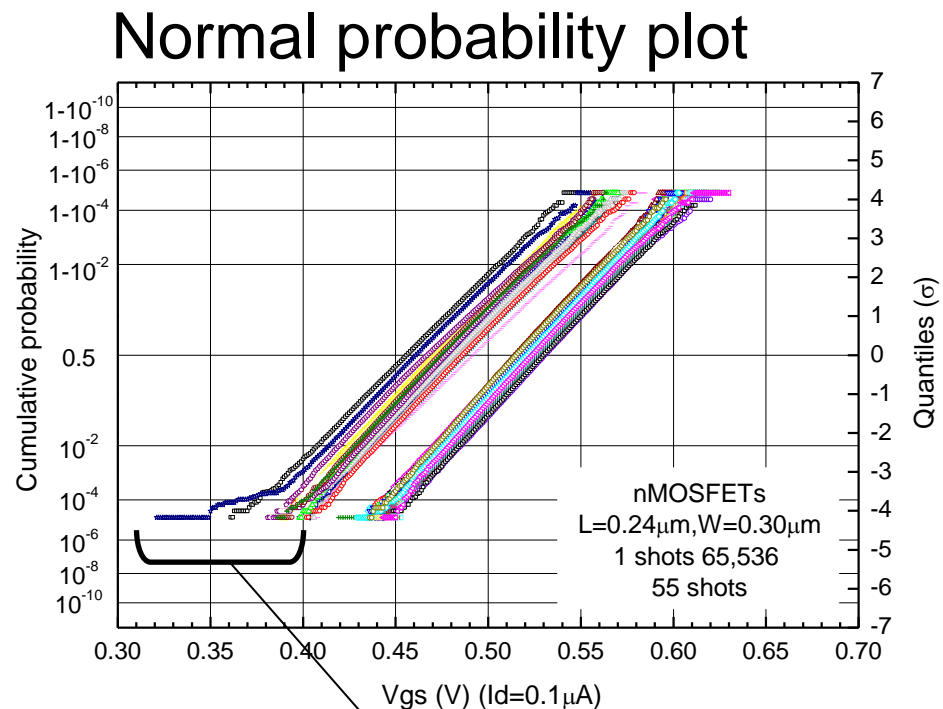
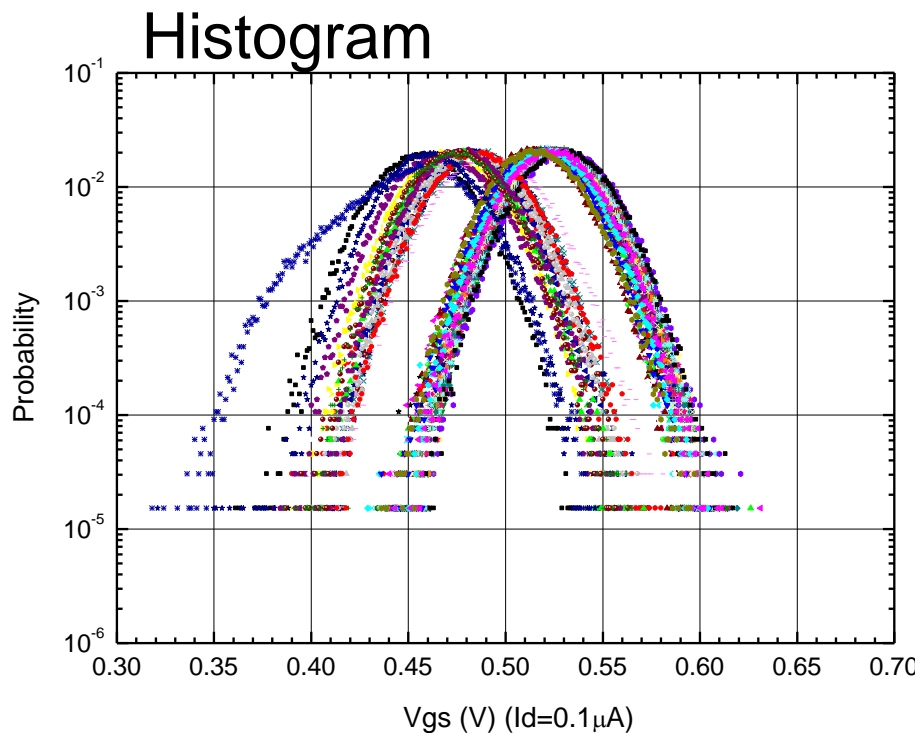
200 mm wafer



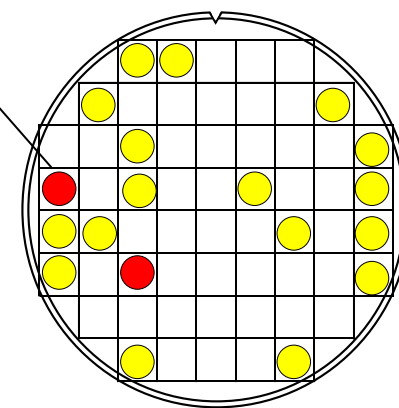
Gate length L (mm)	Gate width W(mm)	Number of transistors
0.22	0.28	65,536 (64x1024)
0.22	0.30	65,536 (64x1024)
0.24	0.30	65,536 (64x1024)
0.24	1.5	65,536 (64x1024)
0.24	15	16,384 (64x256)
0.40	15	16,384 (64x256)
0.40	1.5	65,536 (64x1024)
1.2	0.30	32,768 (32x1024)
1.2	1.5	32,768 (32x1024)
4.0	0.30	32,768 (32x1024)
4.0	1.5	32,768 (32x1024)
0.24	0.30	32,768 (32x1024) Antenna ratio 100
1.2	15	8,192 (32x256)
4.0	15	8,192 (32x256)
10	15	4,096 (16x256)
0.24	0.30	4,096 (16x256) Antenna ratio 1,000
0.24	0.30	1,344 (32x42) Antenna ration 10,000

S. Watabe, et al., *IEEE Trans Electron Devices*, vol. 57, p. 1310, 2010.

V_{th} Variability in a wafer

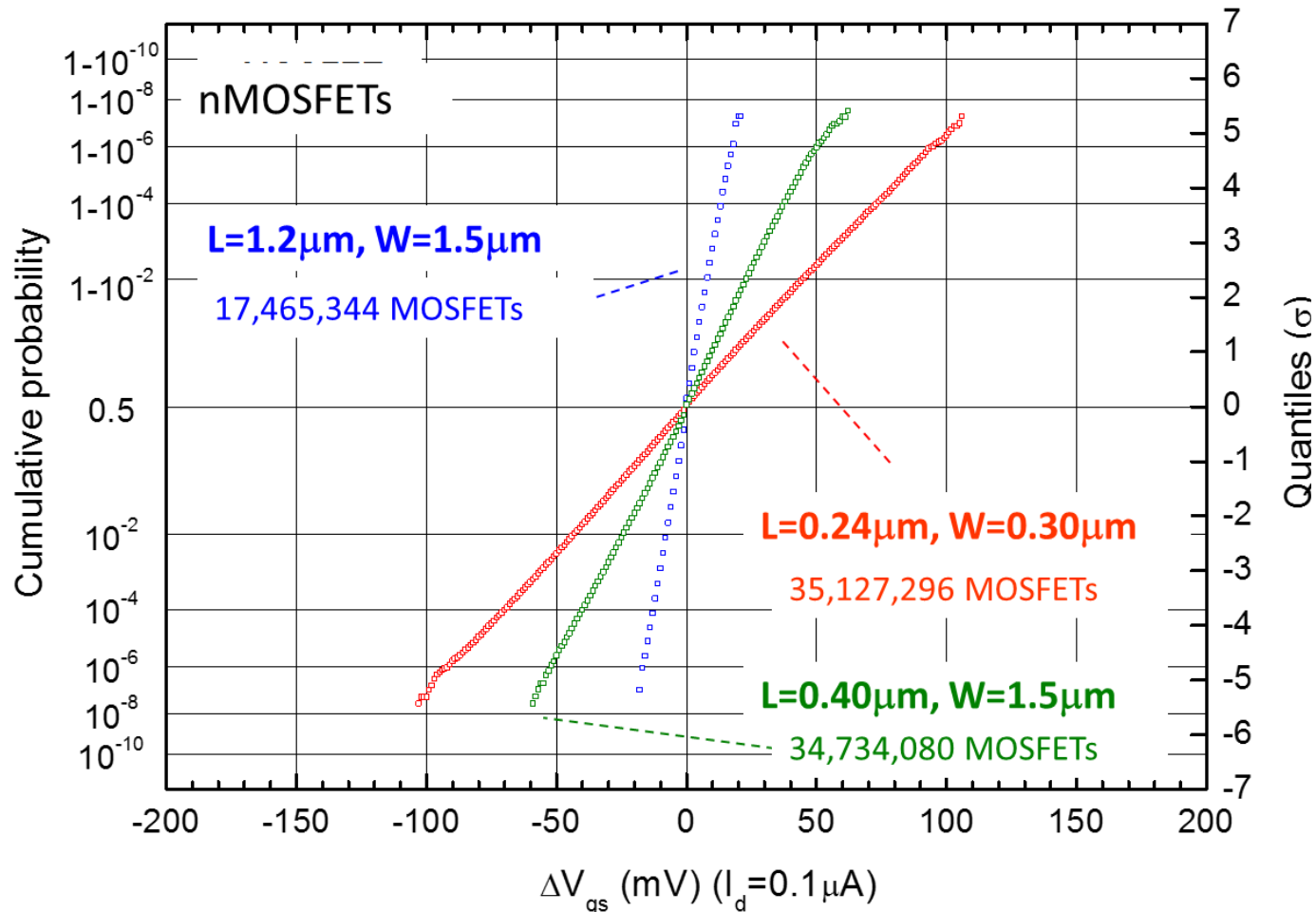


- ~300mV in a 200 mm Φ -wafer
 - ~160mV in a shot
 - ~80mV –Difference between the average V_{th} shot to shot
- Variability in a shot \gg shot to shot



V_{th} Variability dependence on Gate size

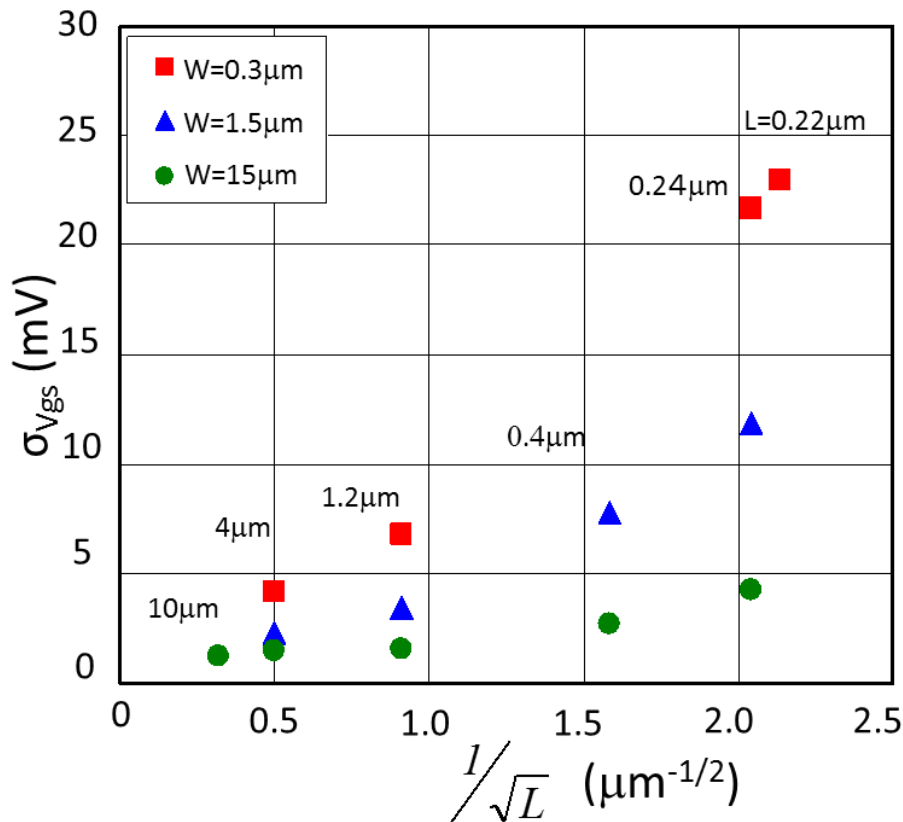
35,000,000 MOSFETs are evaluated



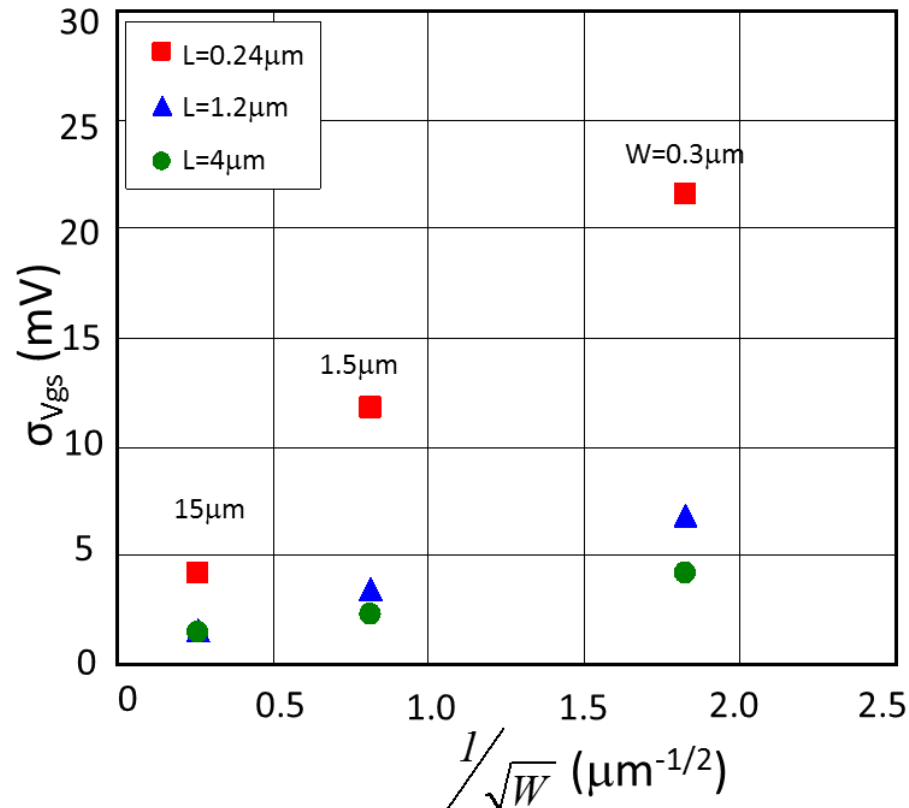
The V_{th} Variability follows the Normal distribution even in the tail part.
(35 Million MOSFETs, $\pm 5.5s$)

V_{th} Variability dependence on Gate size

Gate length

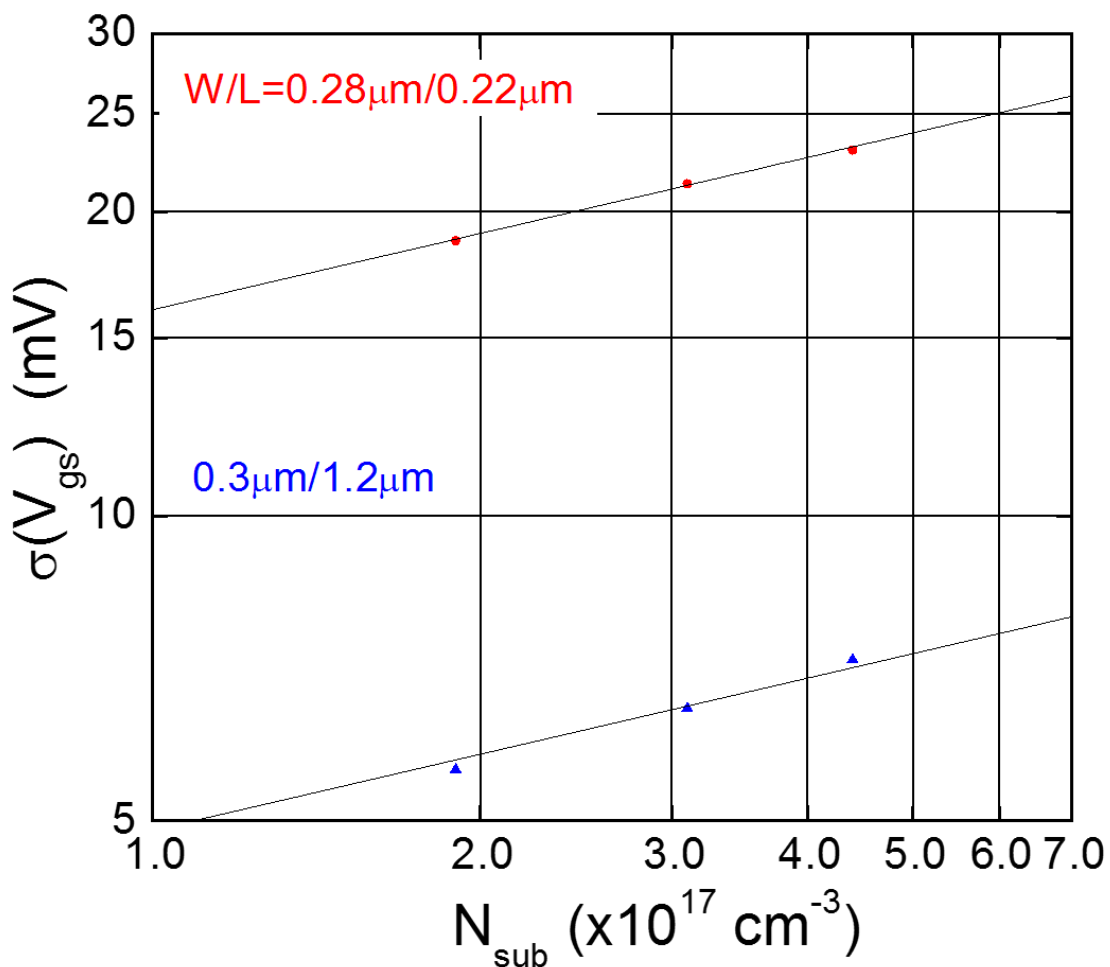


Gate width



Variability increase with an increase of gate length and width.
 $L < 0.4\mu\text{m}$: Variability drastically increases.

Dependence of σ on impurity conc.



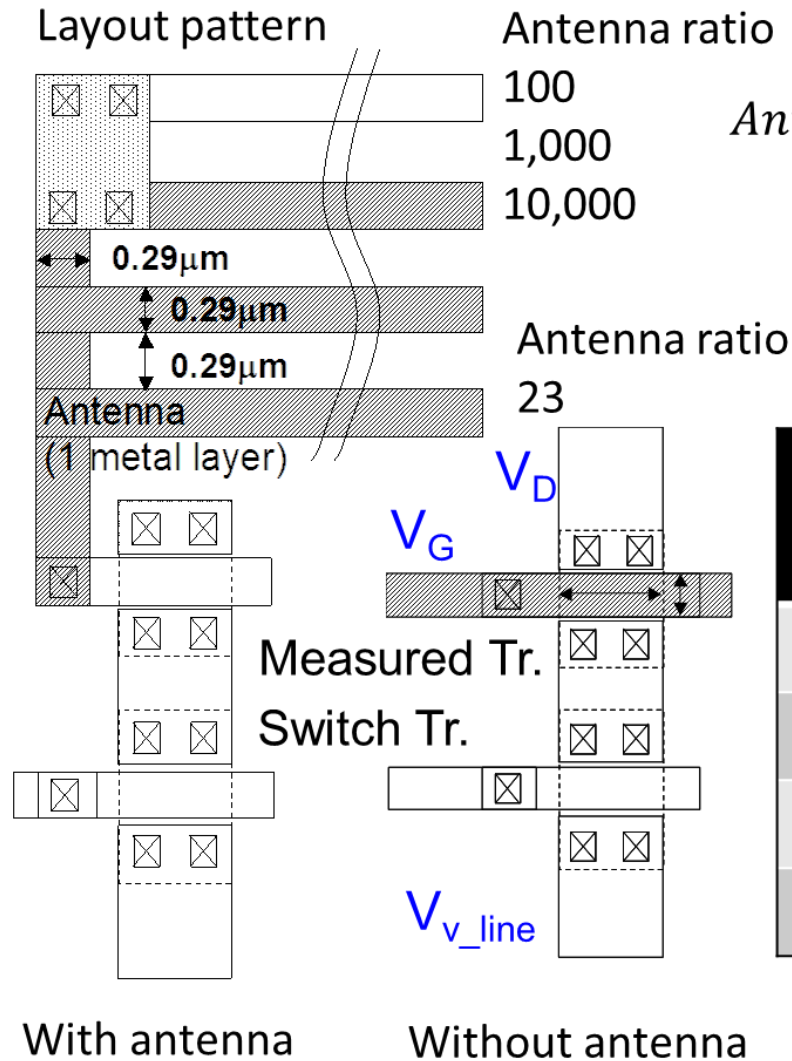
$$\sigma_{V_{th}} \approx \frac{1}{\sqrt{LW}} \left(\frac{4\sqrt[4]{q^3 \epsilon_s \phi_B N_d}}{\sqrt{2}} \right) \frac{T_{ox}}{\epsilon_{ox}}$$



$$\sigma_{N_{sub}} \propto \sqrt{N_{sub}}$$

$$\text{Depletion region} \propto \frac{1}{\sqrt{N_{sub}}}$$

MOSFETs Characteristics Change by Plasma Processes

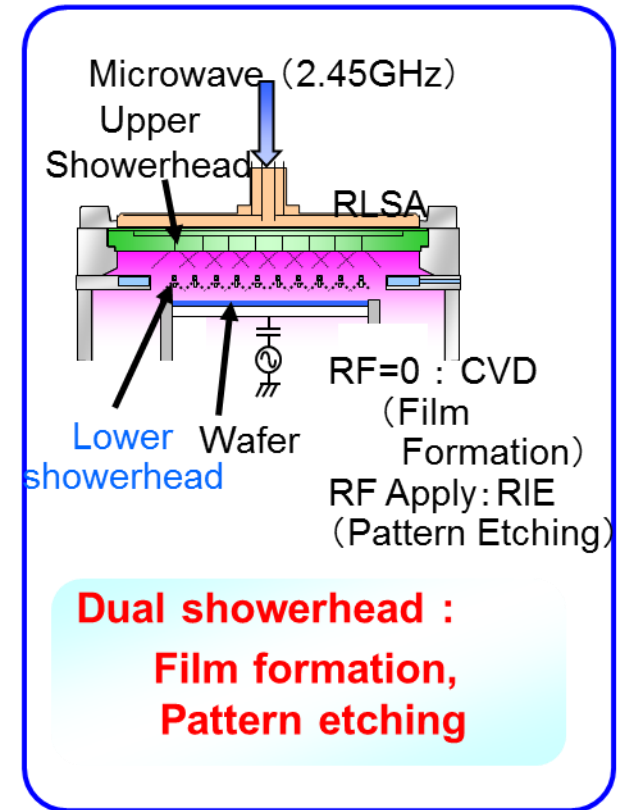
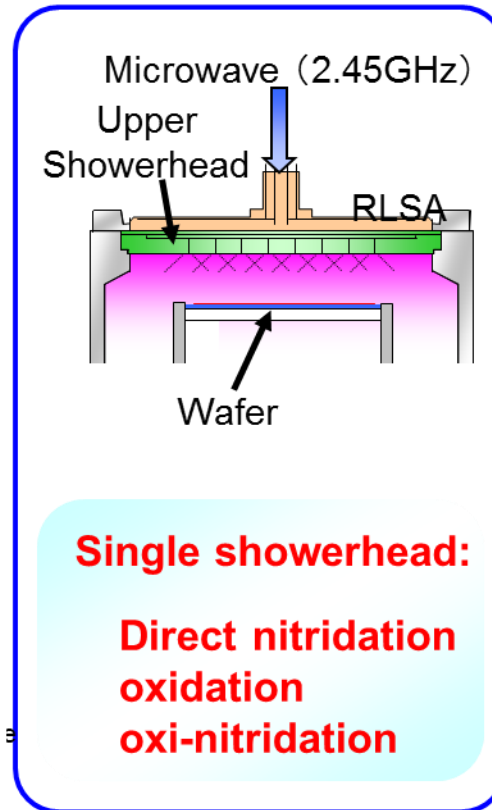
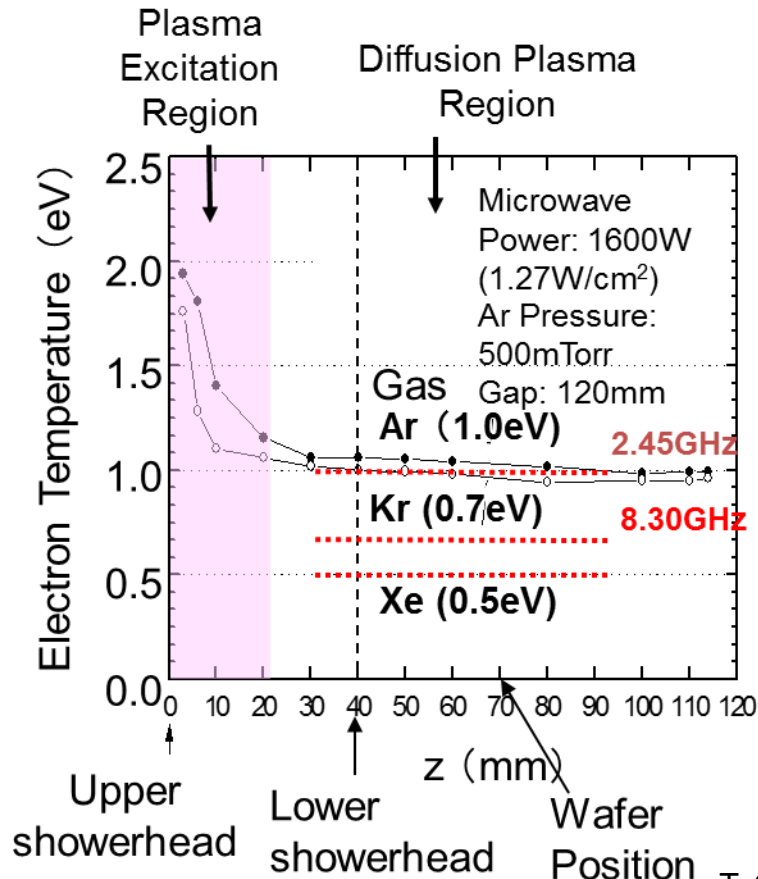


$$\text{Antenna Ratio} = \frac{\text{Area of 1st Metal Layer}}{L \times W \text{ of MOSFET}}$$

Antenna Ratio	Number of MOSFETs	
	NMOS	PMOS
23	65,536	40,960
10^2	32,768	20,480
10^3	4,096	2,560
10^4	1,344	840

Evaluation of Plasma process by antenna pattern

Microwave-Excited High-Density Plasma Equipment with the Single and the Dual-Showerhead Structure



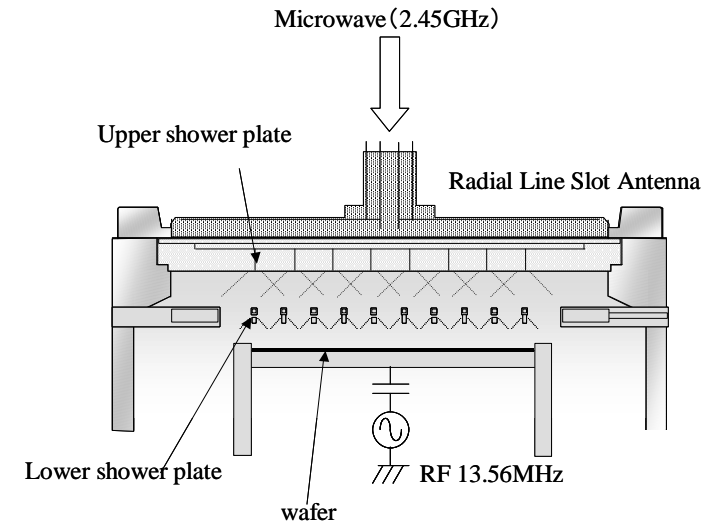
T. Ohmi, M. Hirayama, and A. Teramoto, J. Phys. D: Appl. Phys. **39** (1), R1 (2006).

- Microwave (high frequency) excited plasma → high density
- Process in diffusion plasma region → low damage

Experimental

After Formation of the antenna, the damage of plasma processes were evaluated.

S. Watabe, et al., *IEEE Trans. Electron Devices*, 57, p. 2010.

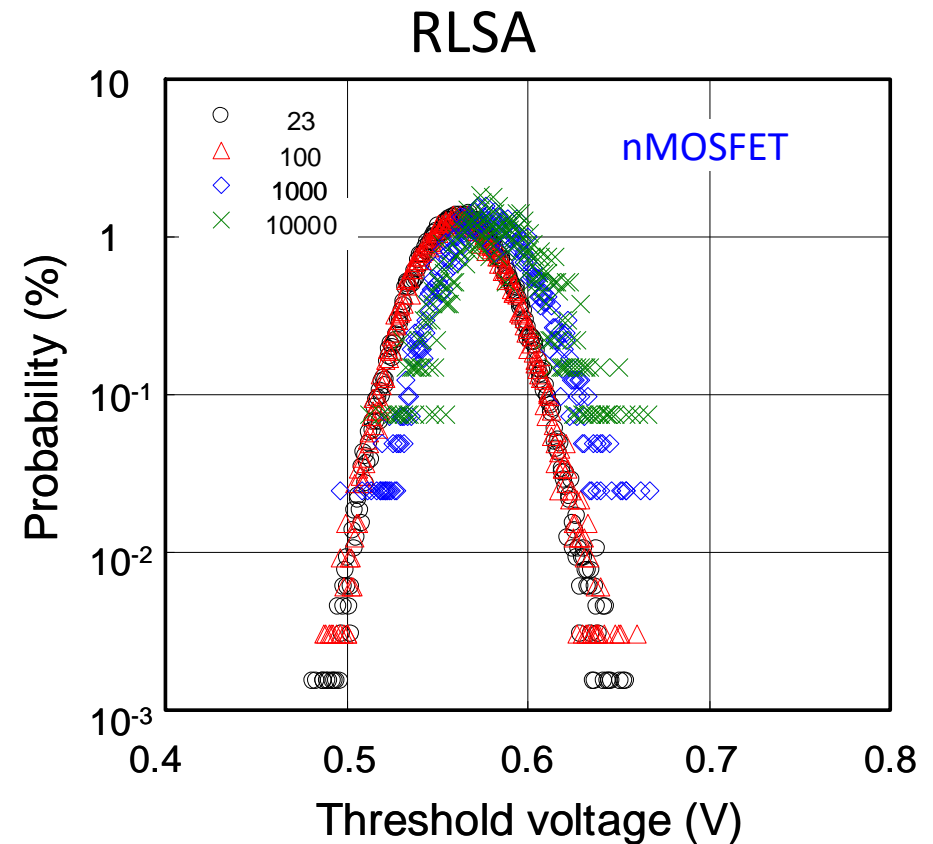
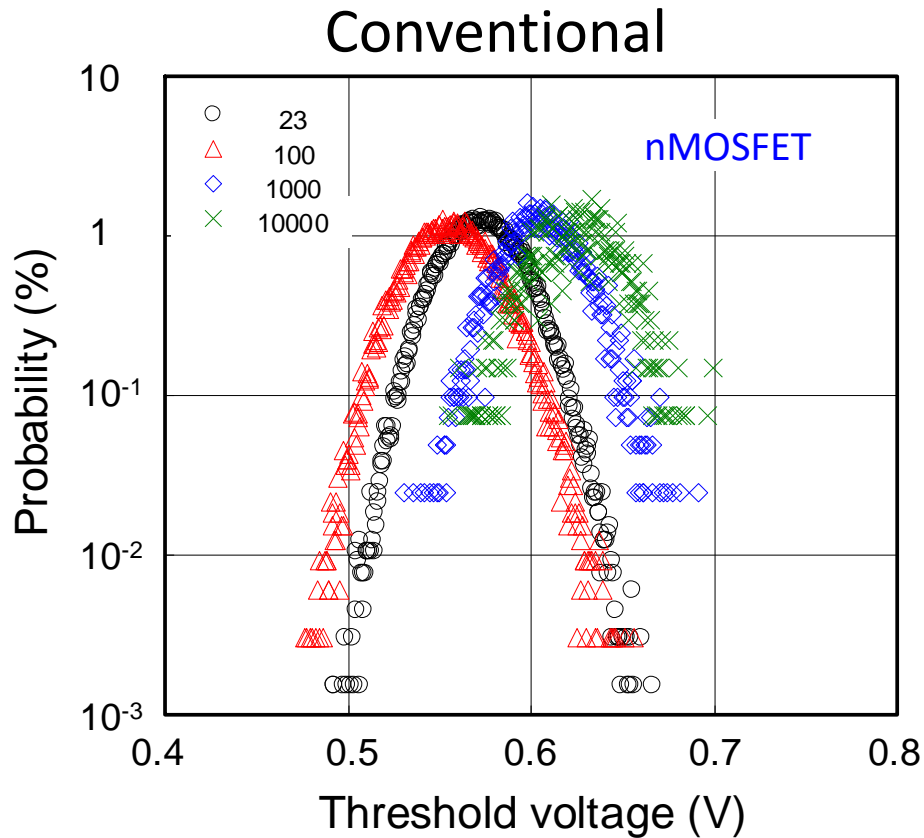


Conventional

RLSA

1st Metal Etching	ECR (Electron Cyclotron Resonance)	RLSA
CVD Interlayer-SiO ₂ Formation M1/M2	ICP (Inductive Coupled Plasma)	RLSA
Via hole Etching interlayer of Metal1-2	Parallel Plate	RLSA

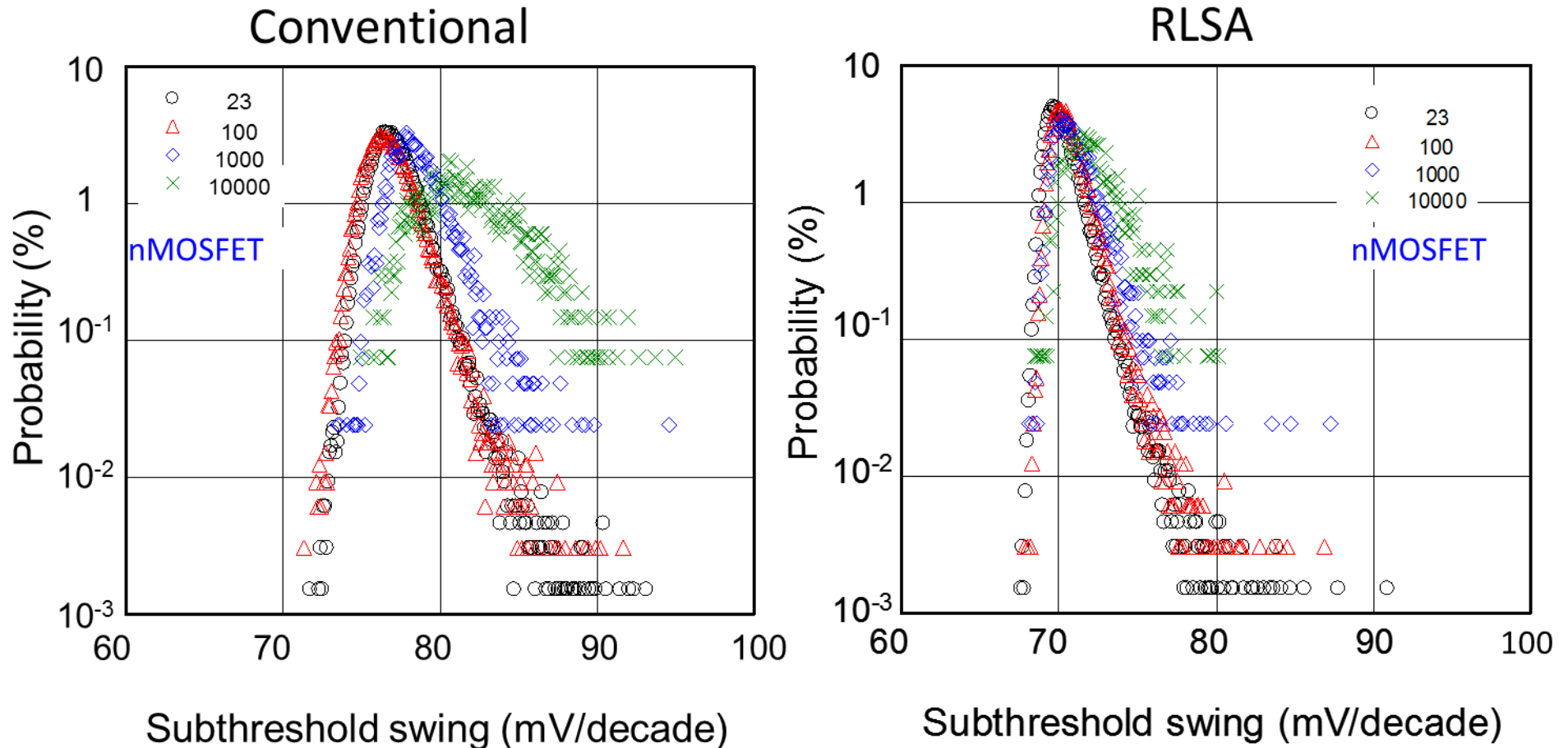
V_{th} Distribution (*n*-MOSFETs)



RLSA Plasma

- V_{th} shift is less than that of conventional.
- No shift less than antenna ratio less than 100.

Dependence of S-factor on antenna ratio(n-MOSFETs)



· By RLSA plasma the average value and variability are improved compared with conventional plasma.

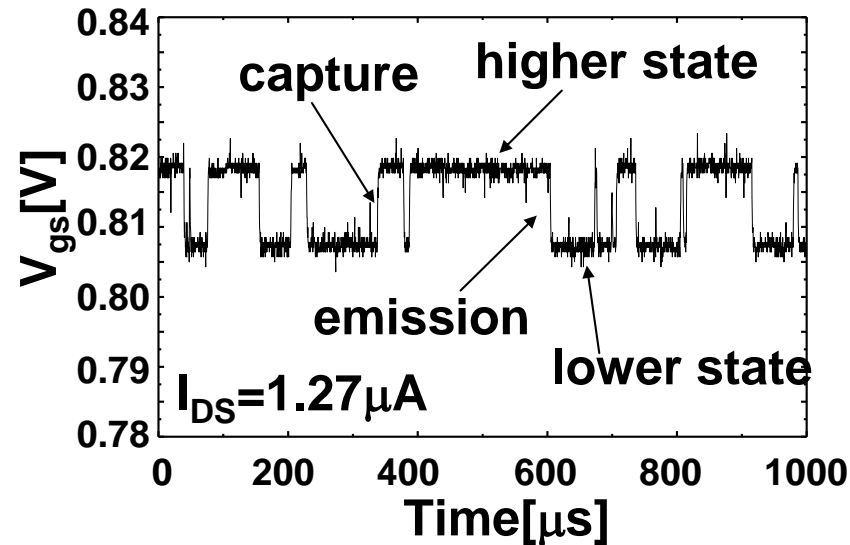
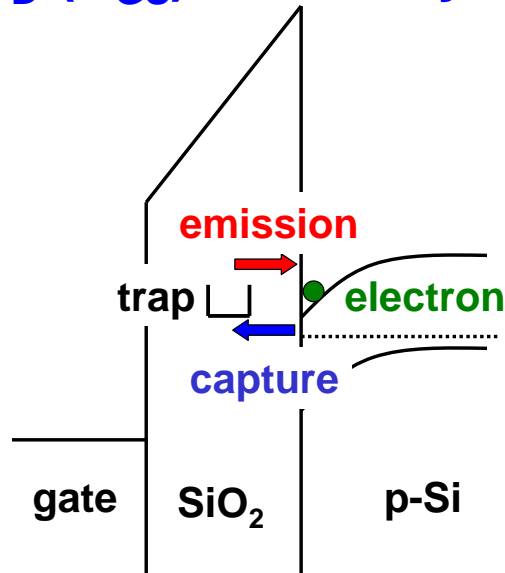
Random Telegraph Noise (RTN)

Random Telegraph Noise (RTN)

Carrier Capture & Emission in Traps in Gate Insulator

⇒ Change of Carrier Number & Mobility

⇒ I_D (V_{GS}) randomly and discretely changes



Increase of RTS by shrinkage of MOS devices causes...

- CMOS Image sensor*

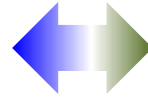
Signal amplitude changes in time domain ⇒ Image Degradation by Twinkle noise

- Flash memory**

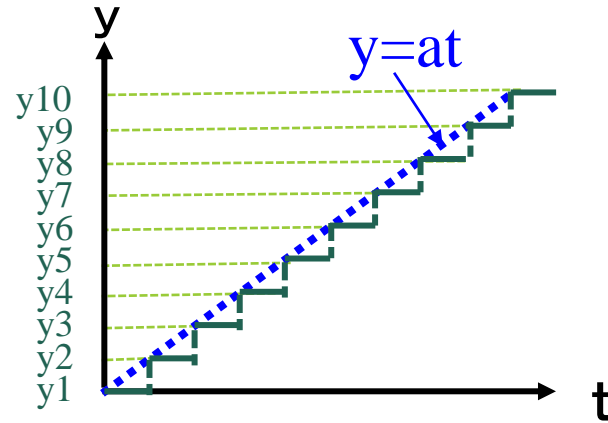
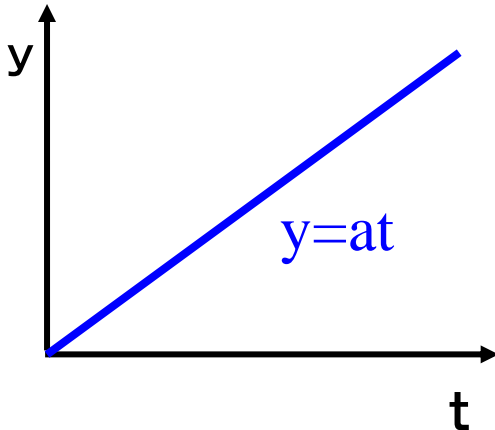
V_{th} variation in read time ⇒ Difficult to multi-bit

アナログ信号とデジタル信号

アナログ信号 : 連続的に変化

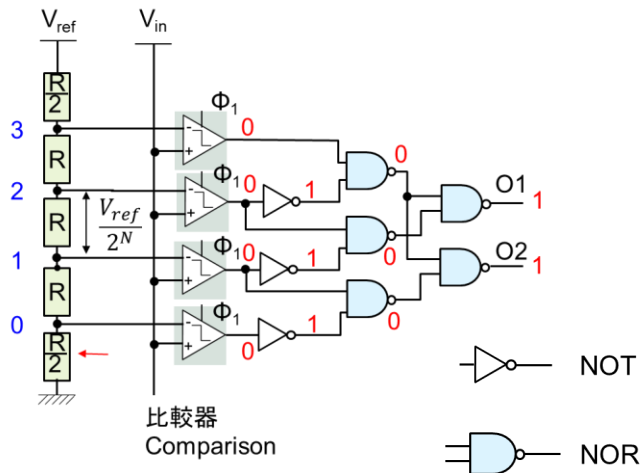


デジタル信号 : 離散的に変化



自然界

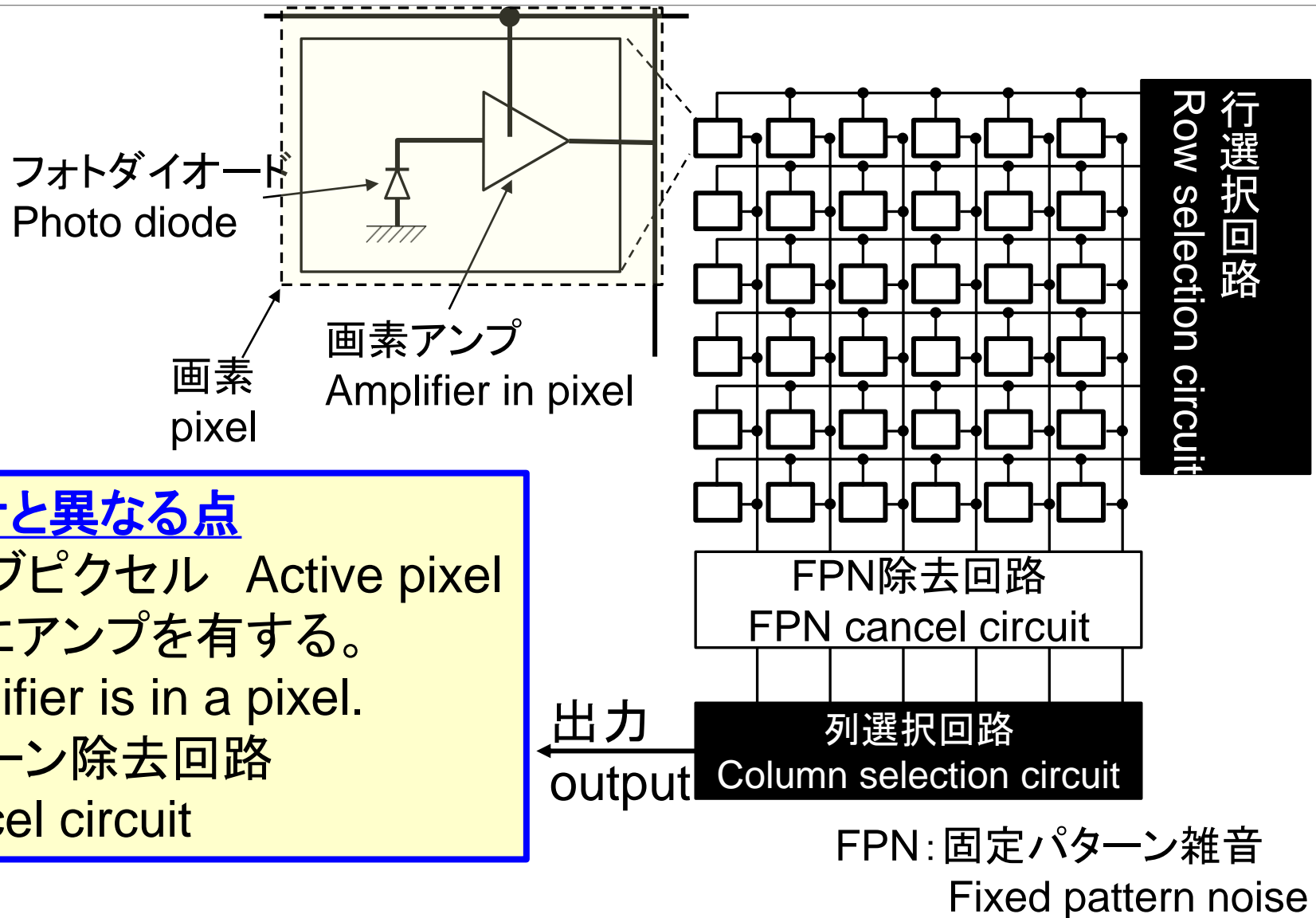
集積回路での演算



NOR

Input		Output
0	0	1
0	1	0
1	0	0
1	1	0

CMOS image sensor



MOSセンサと異なる点

- アクティブピクセル Active pixel
画素内にアンプを有する。
An amplifier is in a pixel.
- 固定パターン除去回路
FPN cancel circuit

RTN Evaluation

Problems in RTS evaluation

- ◆ Appearance Probability of MOSFETs having RTS is relatively small. → Long searching time is required for unit MOSFET measurement.
- ◆ RTS characteristics show large variation for each MOSFETs. Amplitude, time constant, temperature dependence, bias dependence

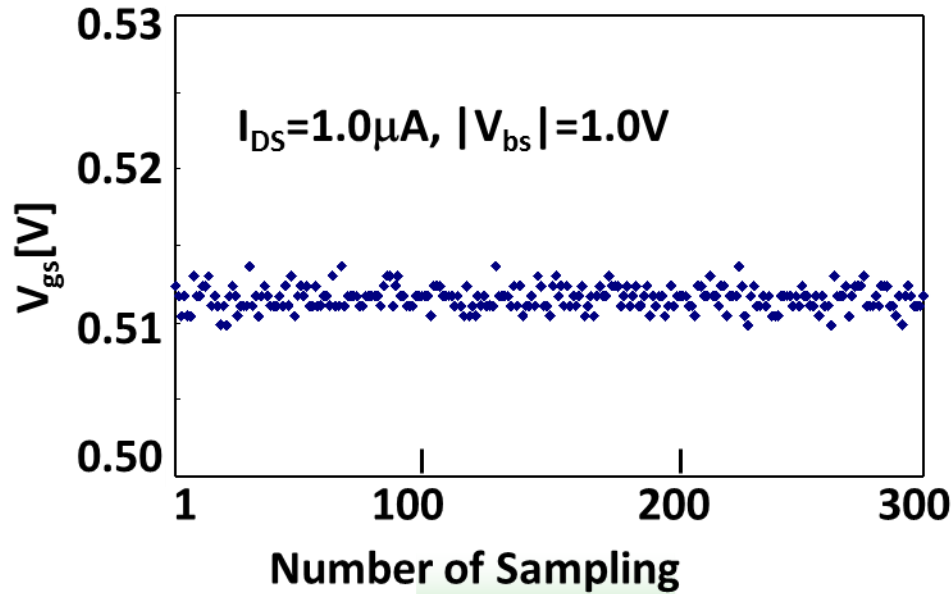
- Location, energy state and cross section of traps
- non-uniformity of channel
(Gate insulator thickness, Localization of impurity atoms)
- Degradation and recovery characteristics for stress

Variation of RTS characteristics

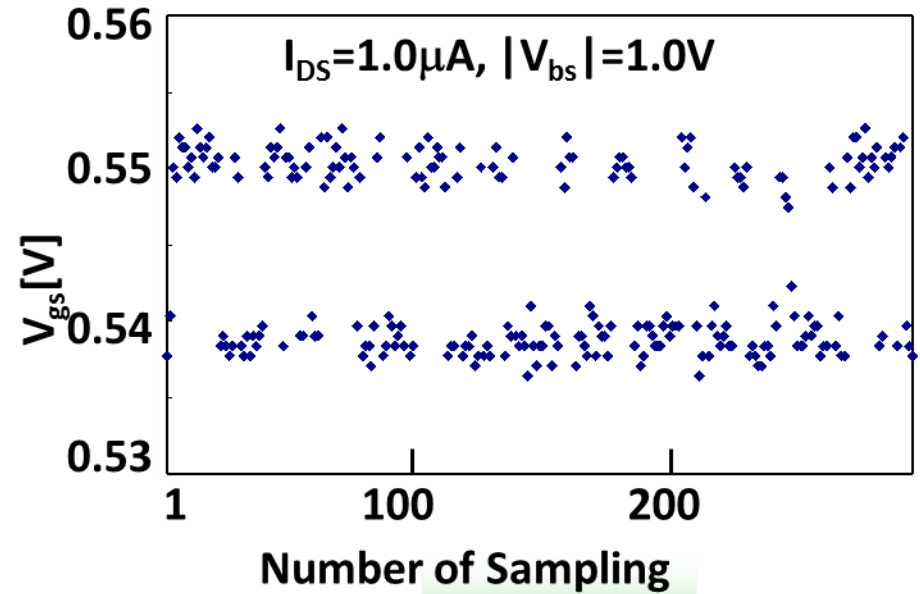
RTS must be statistical phenomenon!!

***It is essentially required that
RTS is statistically evaluated.***

Definition of σ_R – Indicator of RTN

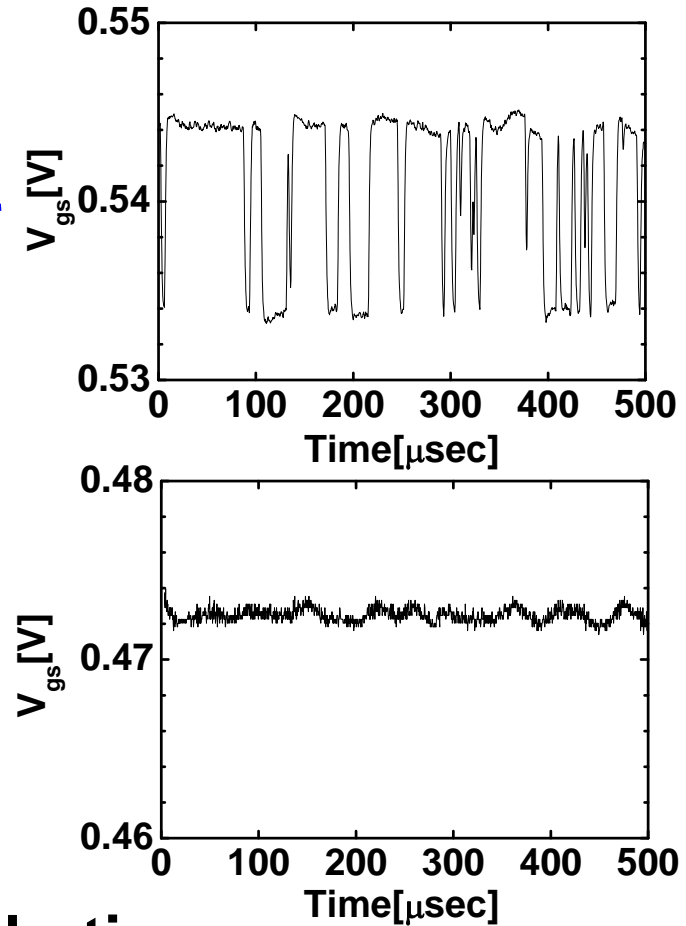
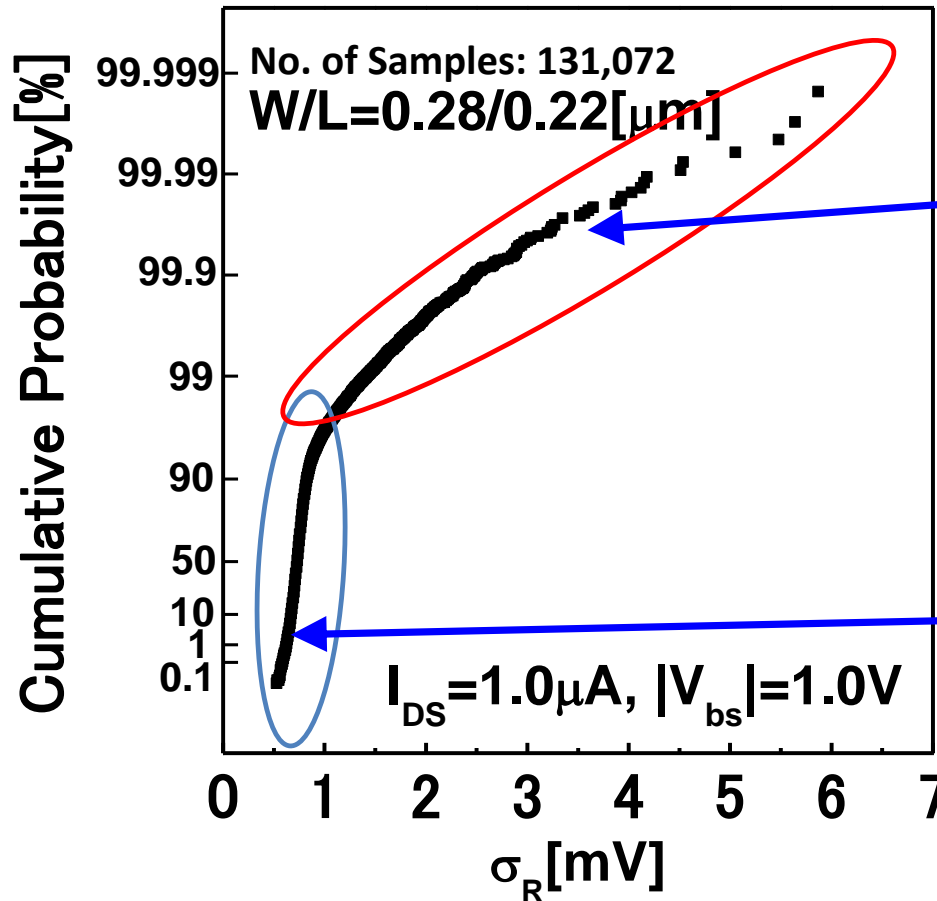


$\sigma_R = 1.15 \text{ mV}$



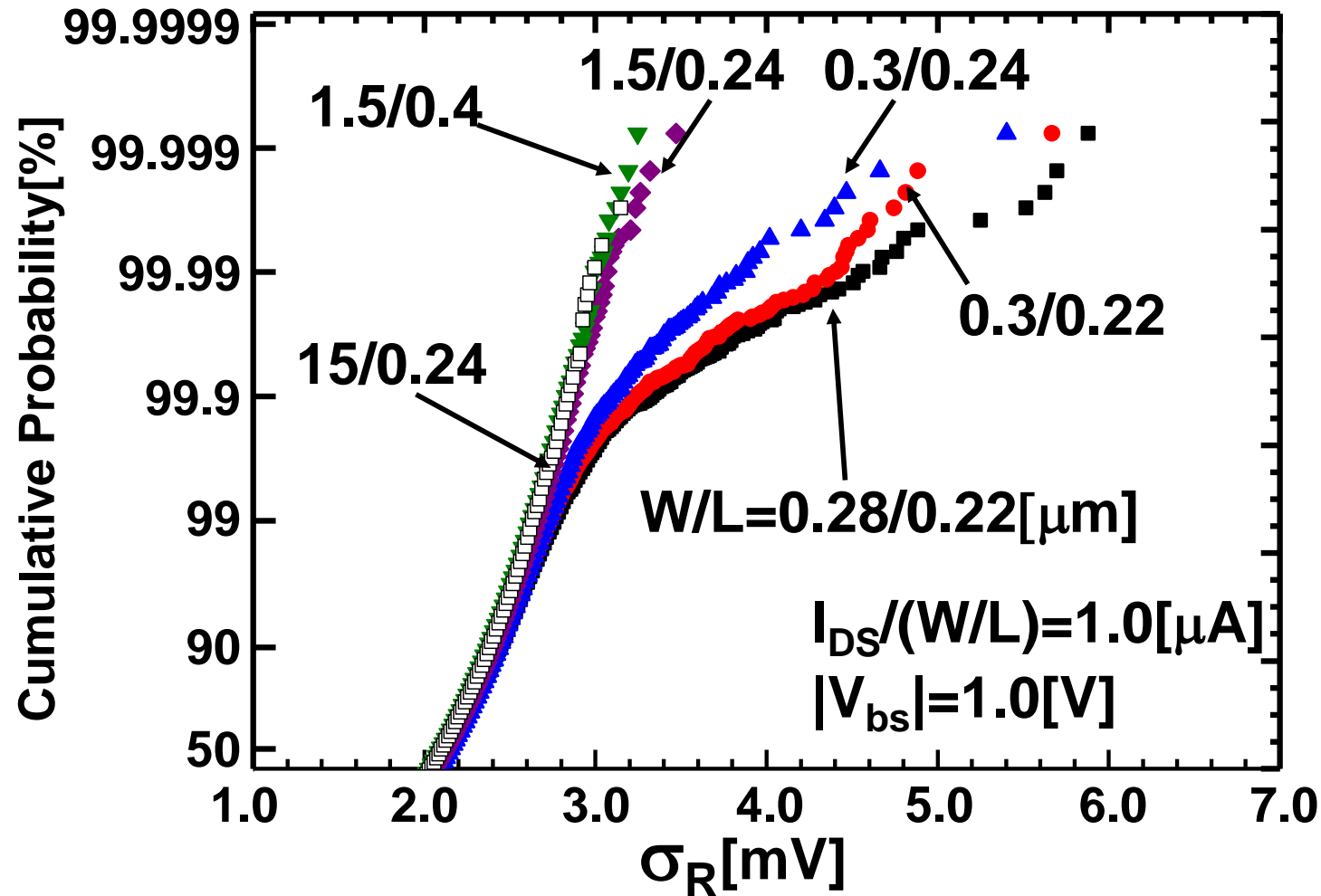
$\sigma_R = 9.09 \text{ mV}$

Relation between RTN waveforms and σ_R Distribution



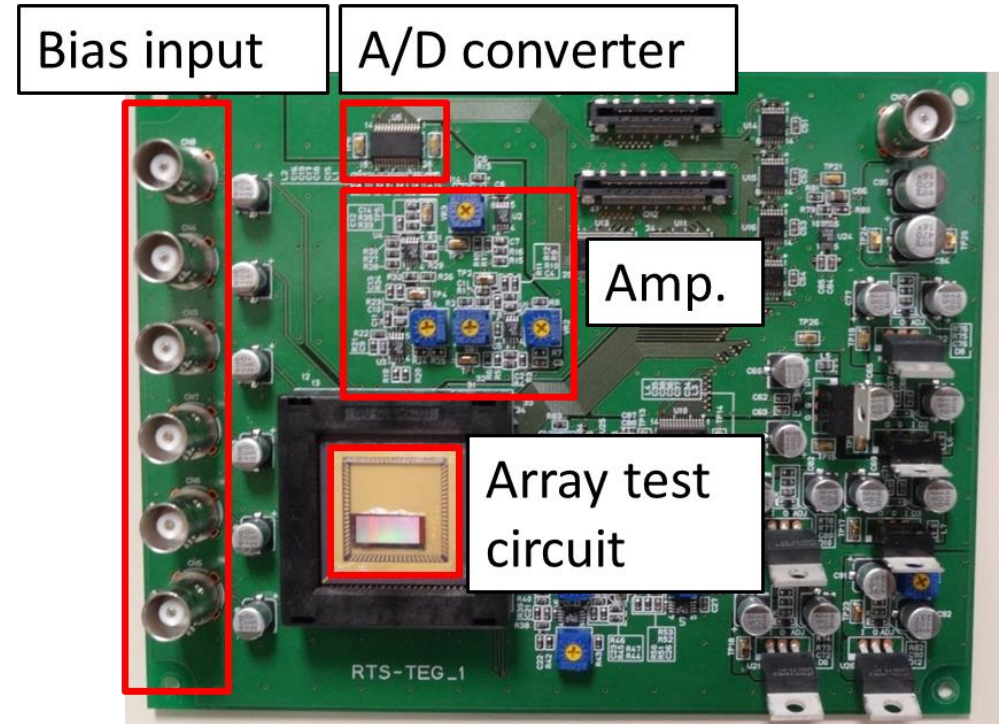
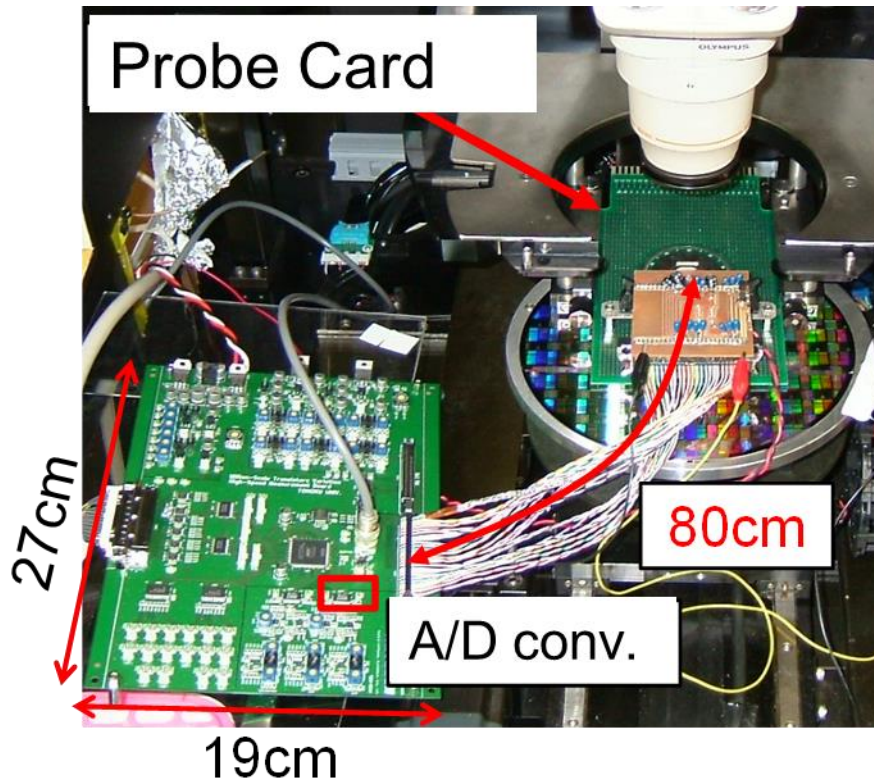
- σ_R distribution is NOT normal distribution.
- A characteristic tail spreads to the right-side. (less than 1 %)
- RTS appears in the tail part.

Gate Size Dependence of σ_R Distributions



Smaller gate size, Larger σ_R tail.
The tails follow Gumbel distribution.

Measurement system & Accuracy



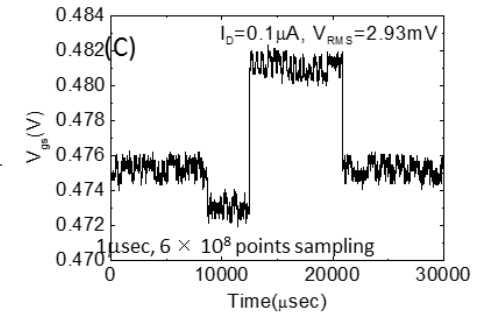
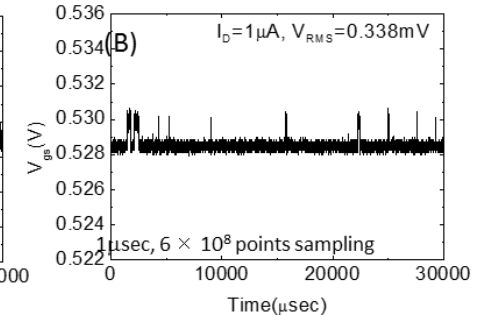
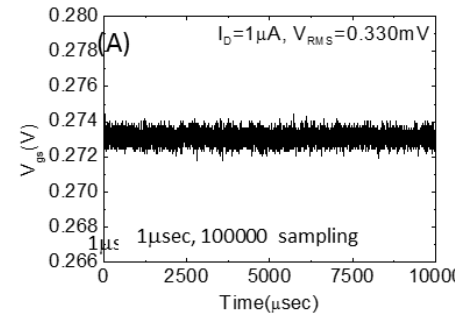
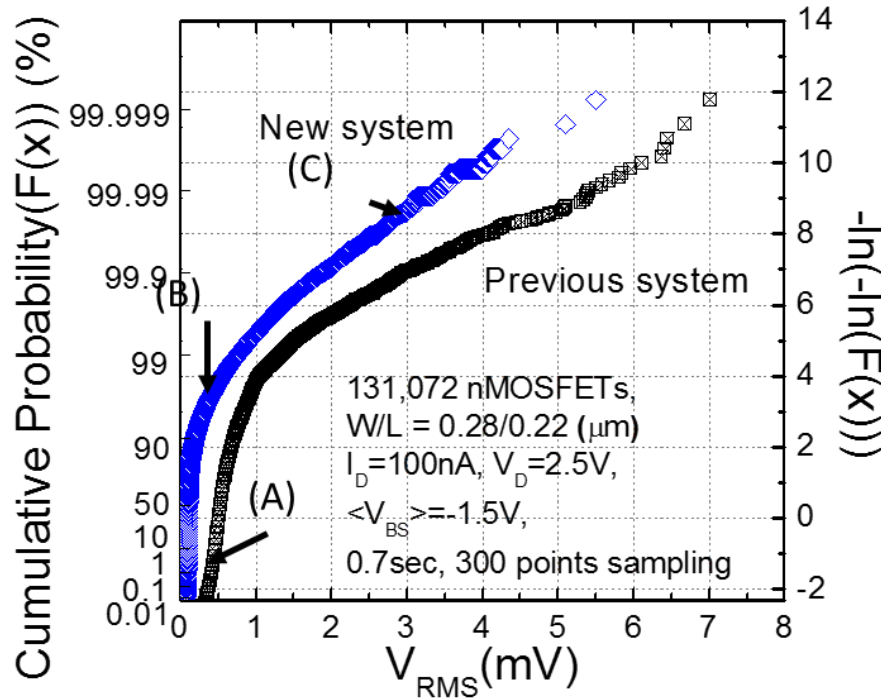
Y. Kumagai et al., Jpn. J. Appl. phys., 50, p. 106701, 2011. S. Watabe et al., Jpn. J. Appl. phys., 46, p. 2054, 2007.
K. Abe et al., VLSI. Technol. symp., p. 210, 2007. A. Yonezawa et al., IRPS, XT-11, 2013.

- ❑ On-Wafer Measurement System
- ❑ On-Board Measurement System

Floor noise **400 μV**
Floor noise **67 μV**

Effect of accurate measurement system

T. Obara, A. Yonezawa et al., SSDM, p.722, 2013.

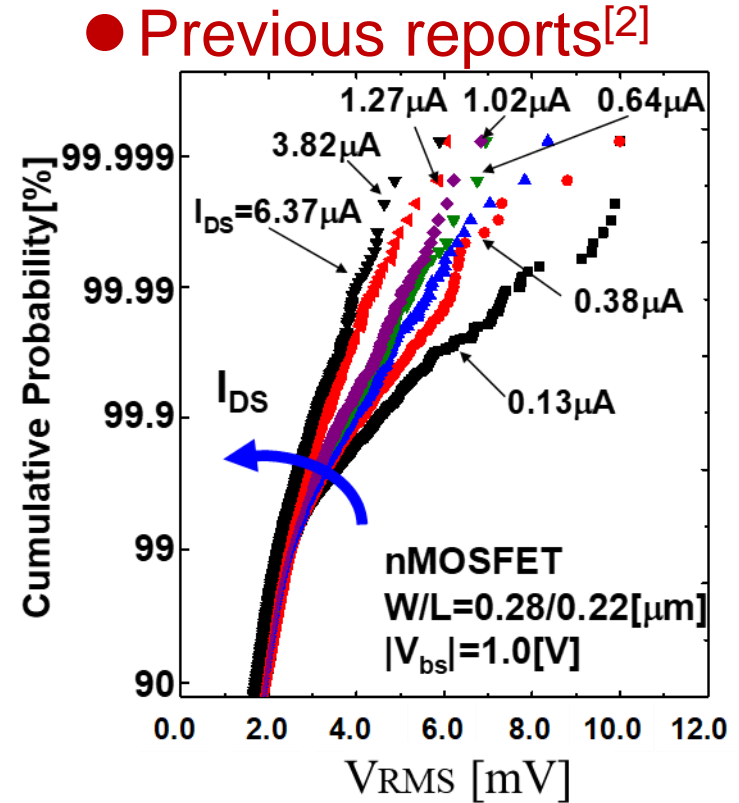
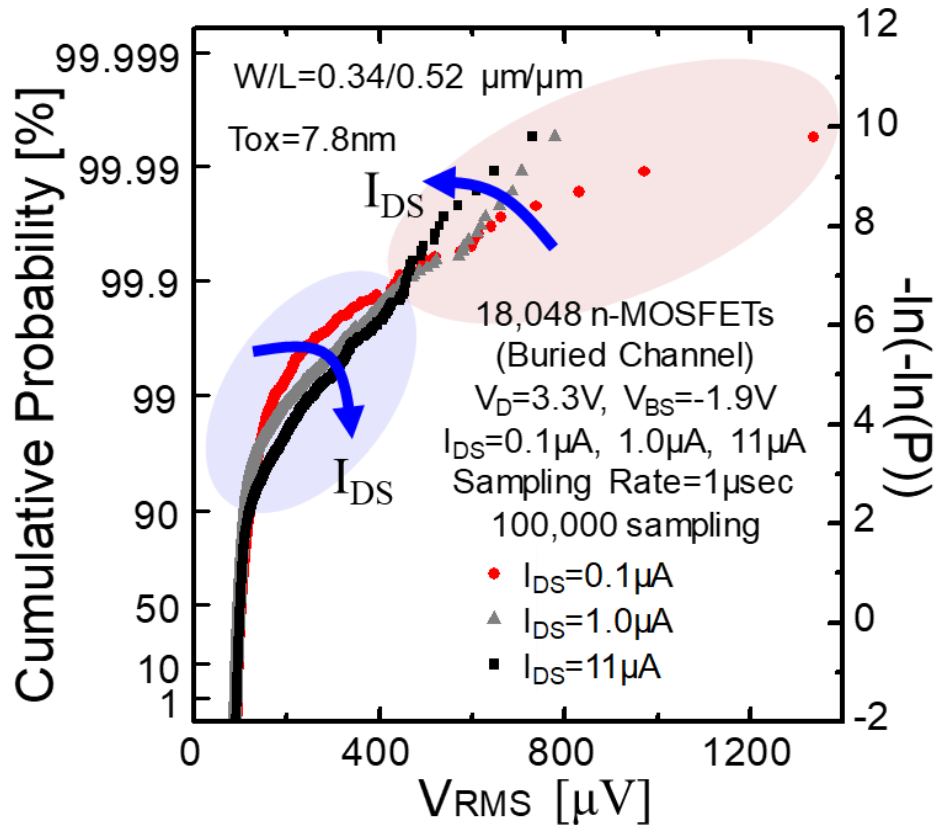


ノイズ強度:

$$V_{RMS} = \sqrt{\frac{\sum_{i=1}^N (V_{OUT,i} - \overline{V_{OUT}})^2}{N-1}}$$

- (B):** We can observe the RTN wave form at the same V_{RMS} as former system.
- (C):** Over 2 states RTN wave form can be observed,
⇒ New system can observe the RTN wave form having low V_{RMS} .

Dependency of Drain Current to V_{RMS}



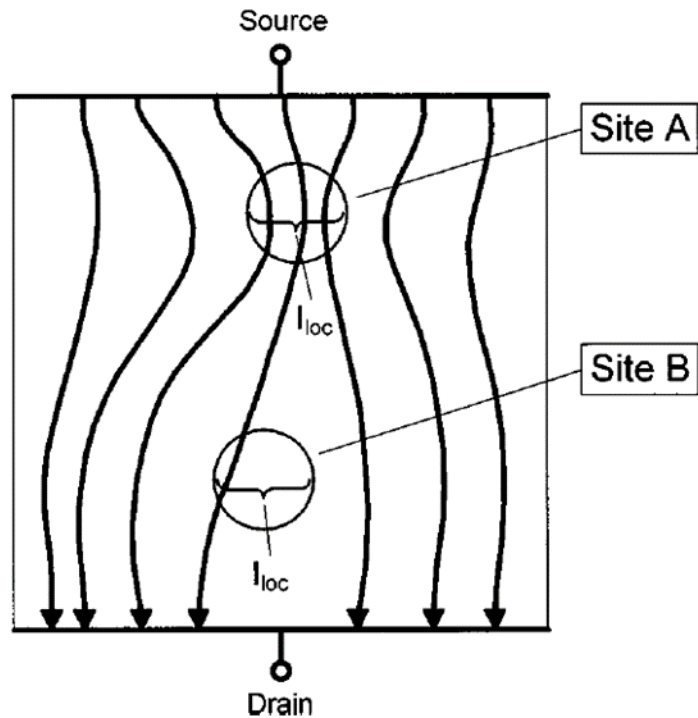
[2] K. Abe, et al., Proc. Int. Image Sensor Workshop, p.62, 2007.

- V_{RMS} in this graph is input referred value at floating diffusion node.
- Cumulative probability of about 99.9%-
 → V_{RMS} becomes larger for smaller drain current.
- Cumulative probability of about 90% - 99.9%
 → V_{RMS} becomes larger for larger drain current.

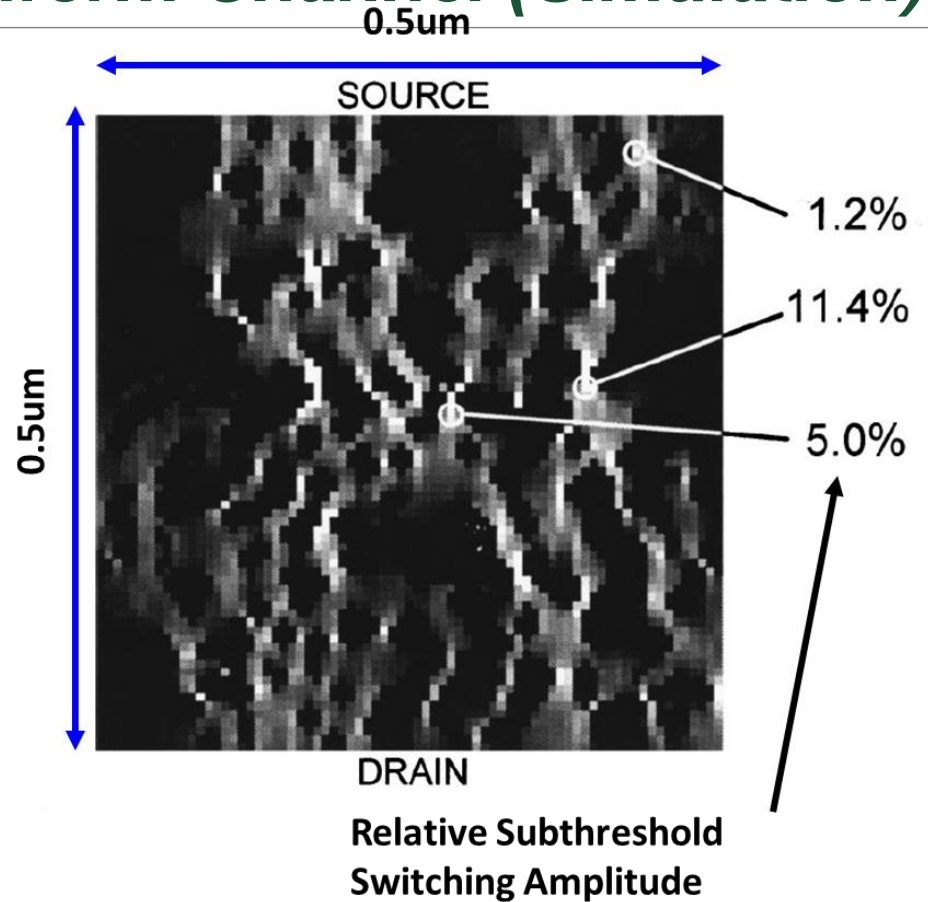
Previous reports*

New data

Amplitude of RTN in Non-Uniform Channel (Simulation)

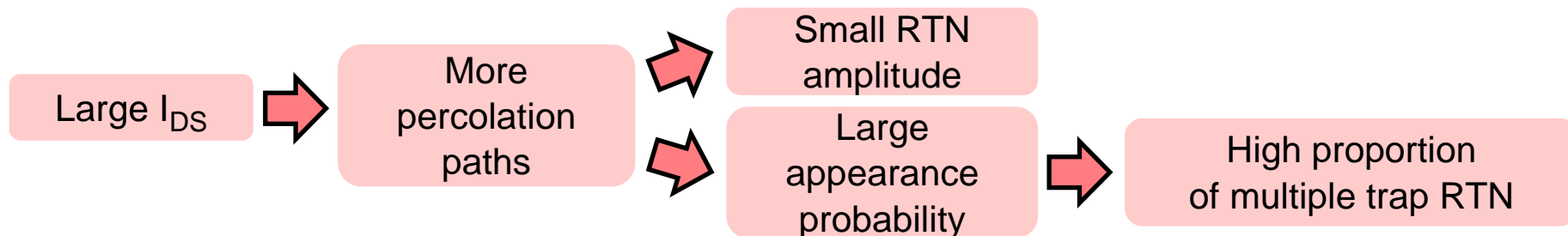
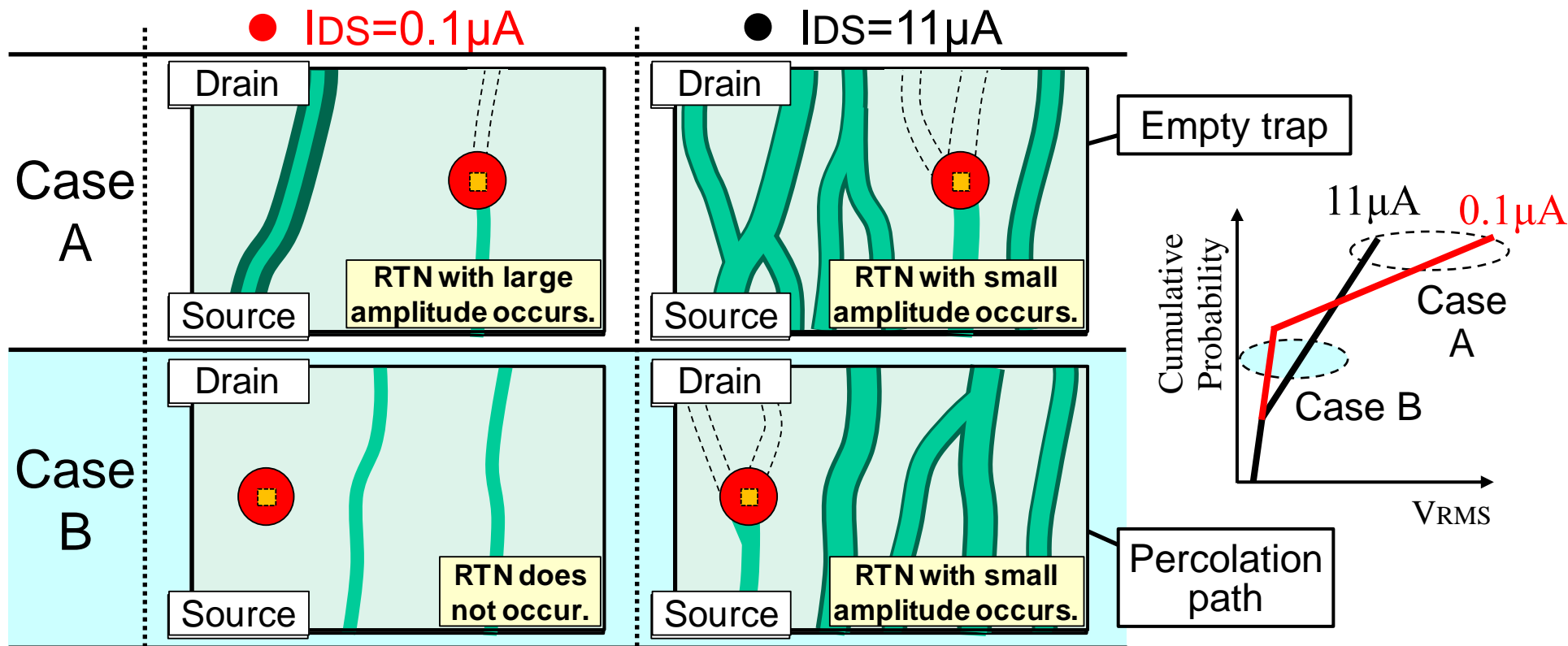


RTS Amplitude: Site A > Site B



H. H. Mueller, et al., "Random telegraph signal: An atomic probe of the local current in field-effect transistors," J. Appl. Phys. Vol.83, pp.1734-1741, 1998

Impact of Drain Current to RTN



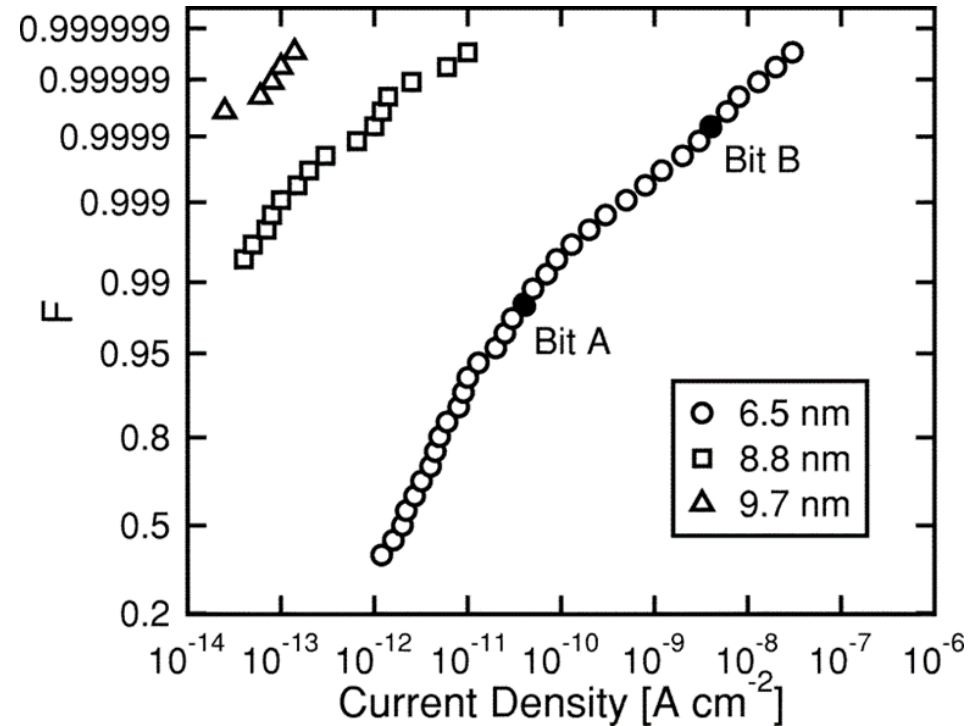
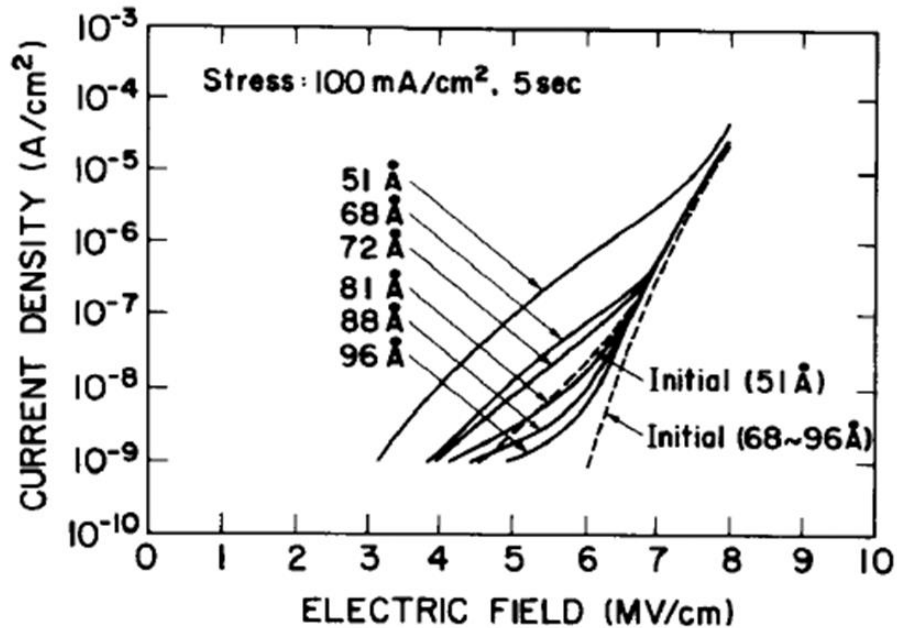
Case A : Impact of the traps to the percolation path increases.

Case B : Probability which traps influence percolation path increases.

絶縁膜のリーク電流

Stress Induced Leakage Current

SILC limits a shrinking tunnel oxide thickness



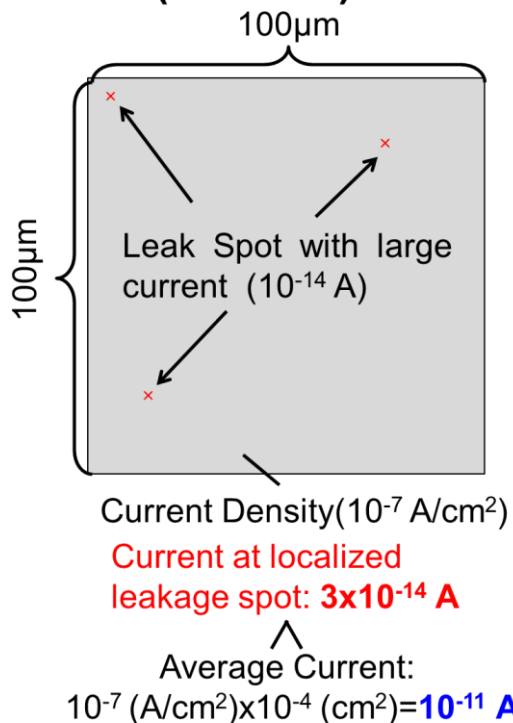
- Stress Induced leakage current (SILC) causes severe bit errors
- Tunnel oxide is thinner, SILC becomes larger.
- Localized leakage spot (trap) indicates large SILC

D. Ielmini, et al., Microelectron. Eng., 59, p.189 (2001).

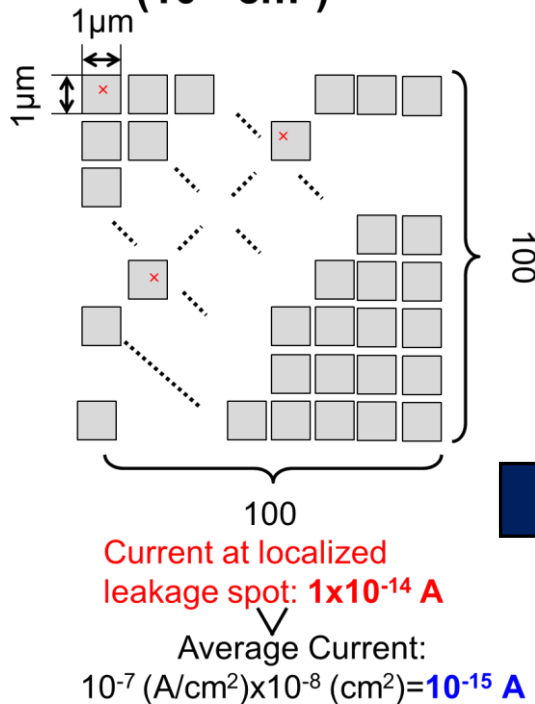
R. Degraeve, et al., IEE Trans. Electron Devices, 51 p. 1392 (2004).

測定への要求

Large Area MOSFET (10^{-4} cm^2)



10000 Small Area MOSFET (10^{-8} cm^2)



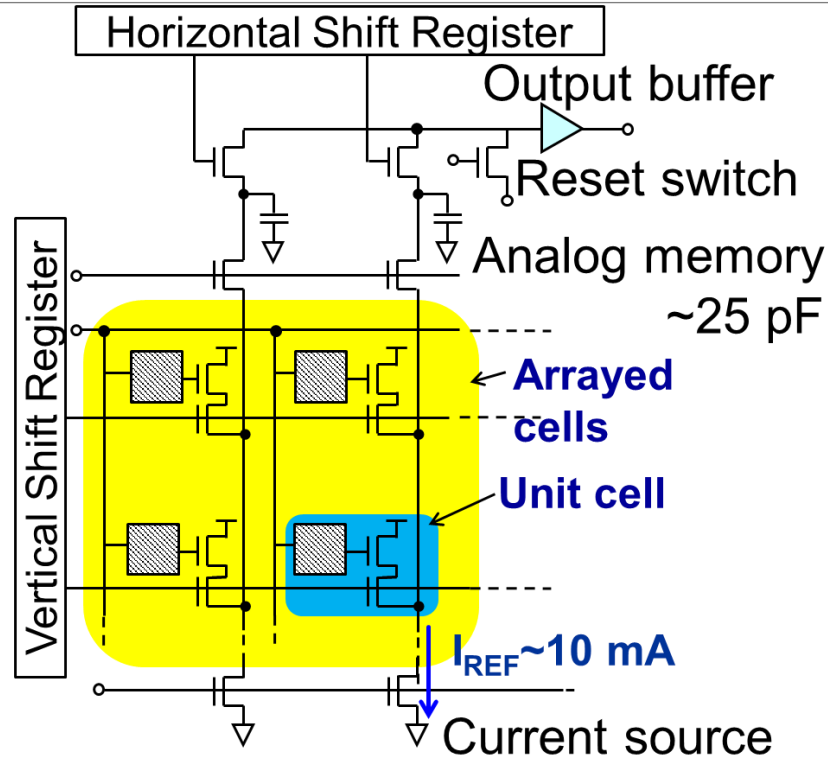
It is essentially required to measure

**- Sufficiently Small Size
- Sufficient number of MOSFETs**

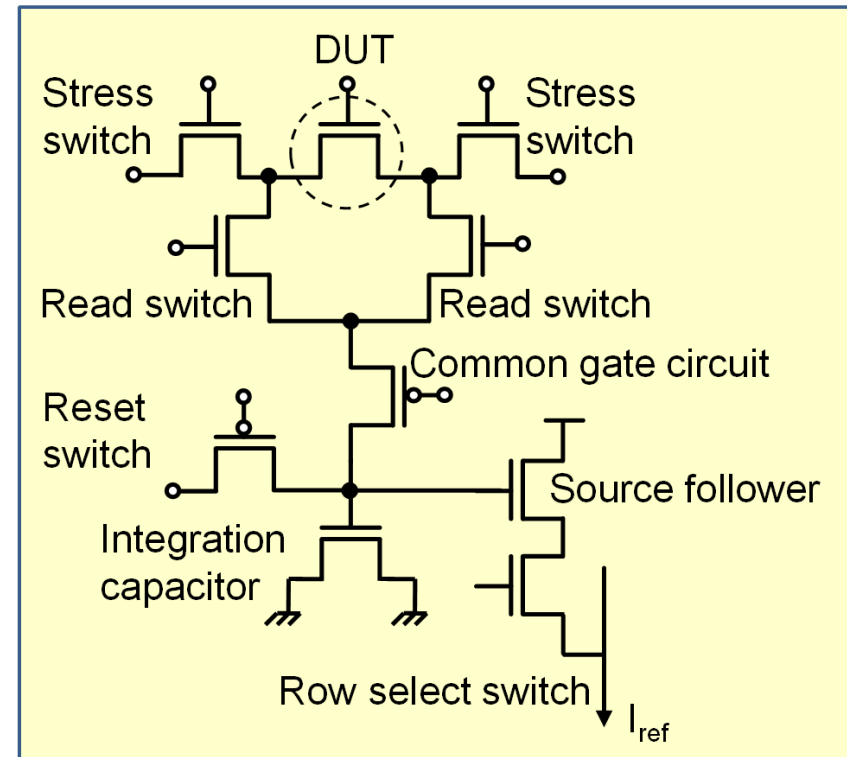
However, Probability : 3/10000, Too small!!

Large leakage current (leakage spot) cannot be detected!

Test pattern for SILC measurement



Unit cell



Sufficient number of DUTs

Unit cells are arranged in matrix pattern $\rightarrow 212^V \times 412^H = 87344/\text{shot}$

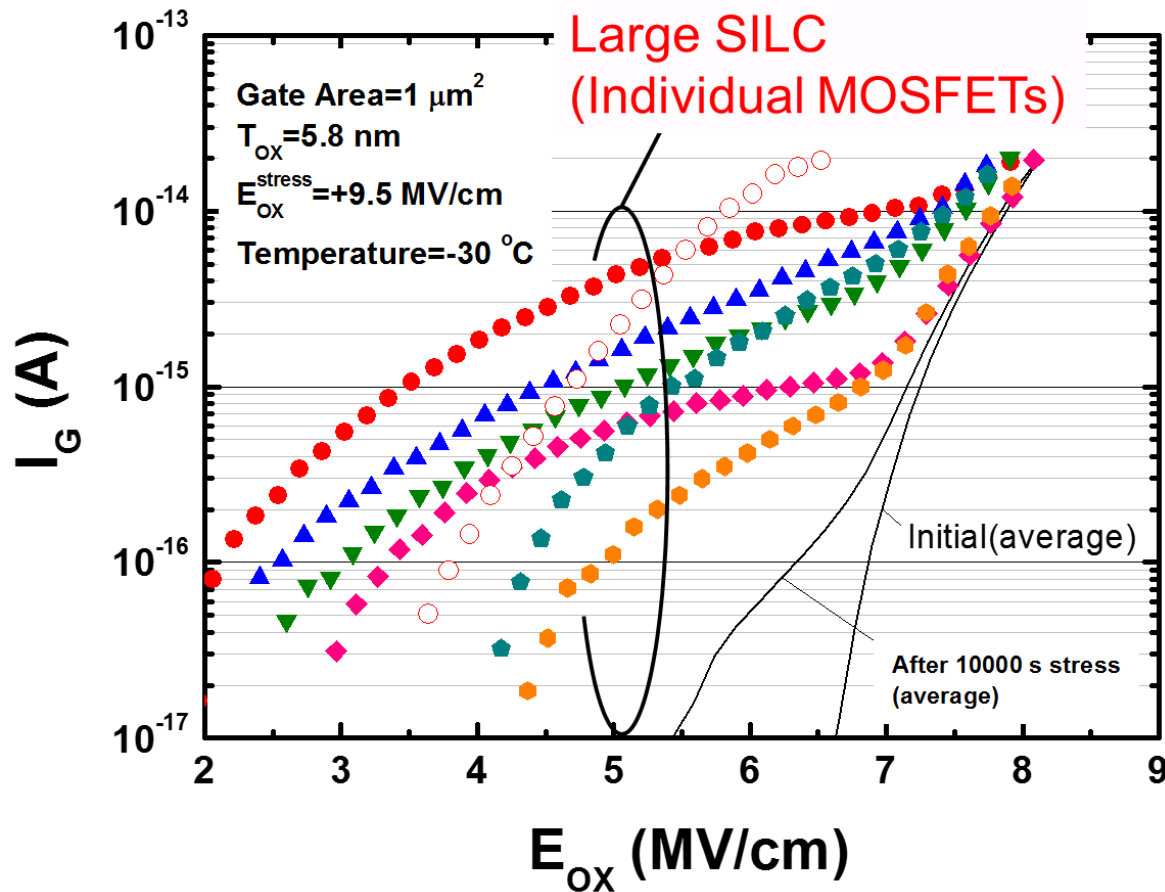
Short integration time and high accuracy

I_G is converted to voltage signal in unit cell by a capacitor ($\sim 14 \text{ fF}$)

High-speed sampling

87344 cells can be measured in 80 sec

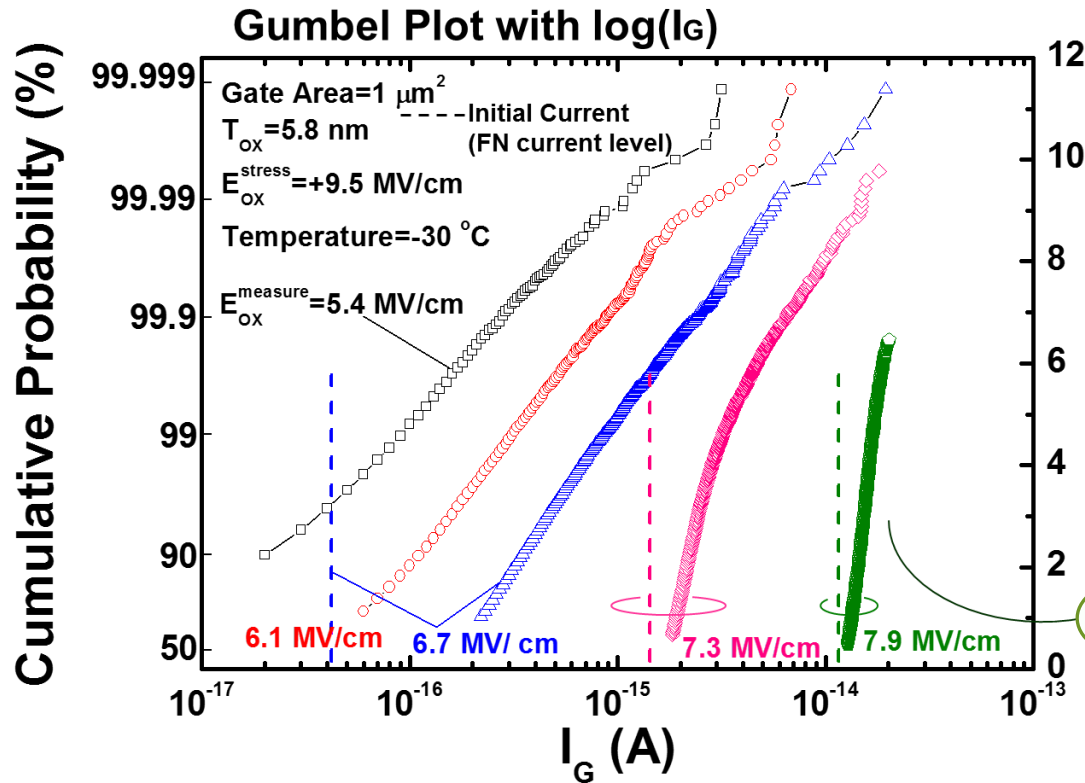
IG-Eox Characteristics of SILC



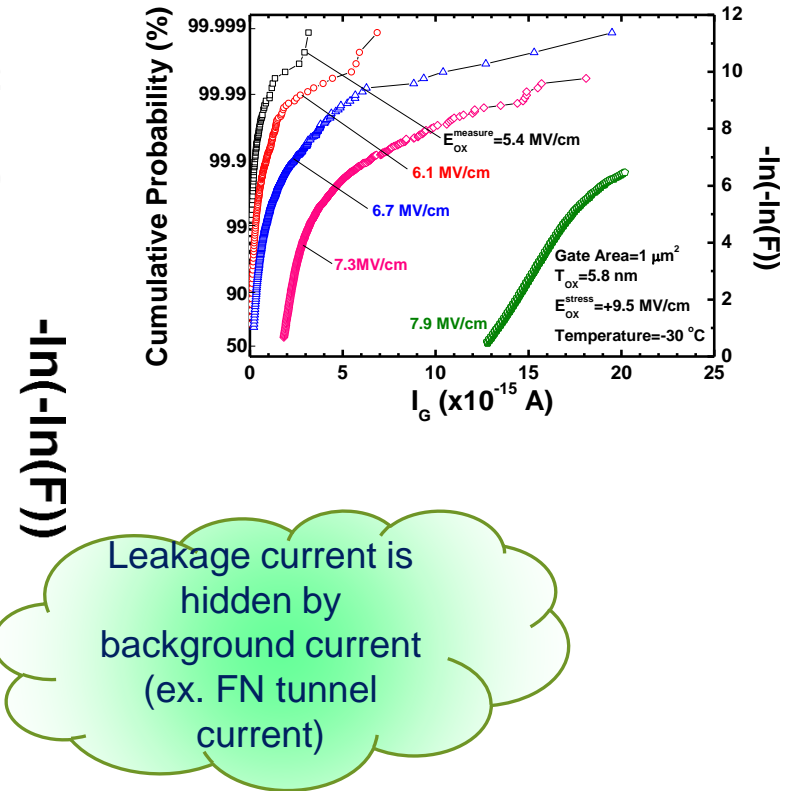
- By evaluation of very low current of 10^{-17} A, a large variety of leakage current can be observed.
- Even at 2 MV/cm, very large leakage current of 10^{-16} A flows the tunnel oxide.

Distribution of SILC

Distribution of SILC



Gumbel Plot with Linear plot (I_G)



Distribution of $\log(I_G)$ (not linear I_G) at low E_{ox} region is on straight line on Gumbel plot. **\rightarrow The leakage current is defined by the current at a leakiest spot.**

半導体デバイス

●Digital/Logicデバイス

デバイスサイズの微細化と高集積化が同時に進行
→デバイスサイズ: Sub-100nmからSub-10nmへ
集積度: 100億-1000億Tr/chip

●Analog・高周波デバイス

Digitalデバイスほど微細化・集積化は進まず
←雑音、バラツキに対して敏感
=デバイスの精度はDigitalデバイス以上のものが求められる。

評価技術: 平均的特性、局所的特性を意識して評価することが重要